Gravity waves from fronts and convection

François Lott, flott@lmd.ens.fr
Laboratoire de Météorologie Dynamique, Ecole Normale Supérieure, Paris

A. de la Camara, D. Cugnet, L. Fairhead, L. Guez, A. Hertzog, F. Hourdin, P. Levan, P. Maury, R. Plougonven, J. Vanneste(+)
(+) University of Edimburgh

1)Impact of Gravity Waves (GWs) on the middle atmosphere dynamics

2)Globally spectral GWs schemes versus multiwave schemes

3)Stochastic GWs scheme and application to convection

4)GWs from fronts via a “smoking gun” approach

5)Tests against observations

Gravity waves from fronts and convection
1) Impact of Gravity Waves (GWs) on the middle atmosphere dynamics

The need to parameterize a broad spectrum of waves: minima of T at the summer mesopause, and closure of the jets an the midlatitudes mesopause (see textbooks, Andrew et al.~1987)

January Temperatures

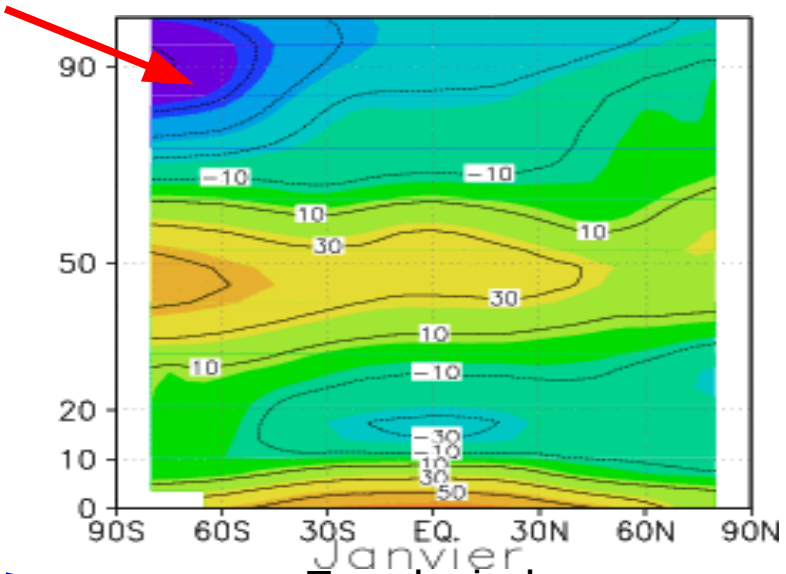

Zonal wind

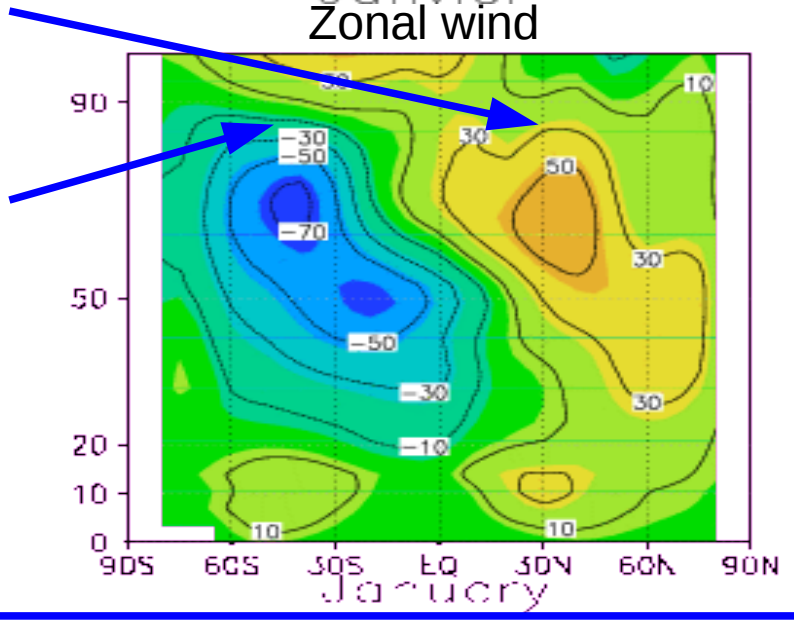

The meridional circulation driven by waves and the « downward control » (review in Haynes et al.~1991)

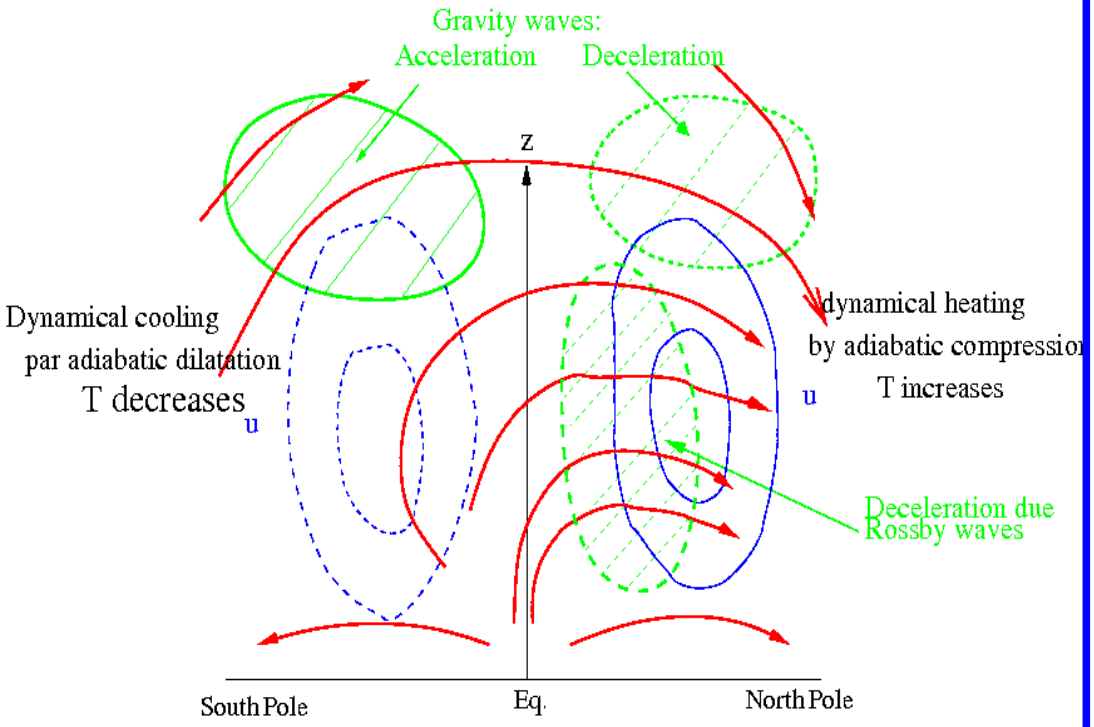

Gravity waves from fronts and convection
1) Impact of Gravity Waves (GWs) on the middle atmosphere dynamics

Presence of westerlies (super-rotation)
In the semi-Annual Oscillation

Zonal wind at the Equator

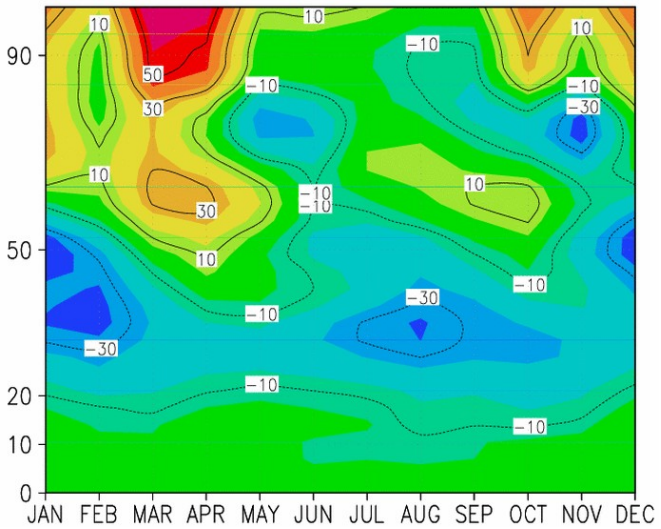

Zonal mean zonal wind as a function of time and altitude (6 years):
tao.atmos.washington.edu

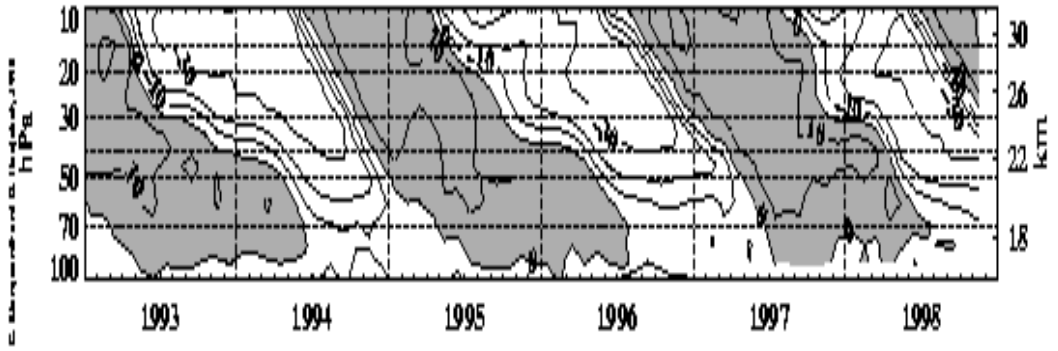

For the role of equatorial waves and gravity waves on the QBO, see Holton and Lindzen (1968, 1972).

For the fast Kelvin waves on the easterly phase of the SAO see Dunkerton (1979)

Gravity waves from fronts and convection
2) Globally spectral versus multiwave parameterization schemes

Subgrid scale parametrizations are based on Fourier series decomposition of the waves field over the model gridbox of sizes δx, δy, and δt (δt can be larger than the model time-step).

$$w' = \sum_a \sum_b \sum_c \hat{w}\left(k_a, l_b, \omega_c\right) e^{i\left(k_a x + l_b y - \omega_c t\right)}$$ a, b, c are integers, (dropped in the following) and $$k_a = a\frac{2\pi}{\delta x}, l_b = b\frac{2\pi}{\delta y}, \omega_c = c\frac{2\pi}{\delta t}$$

Since a lot of waves with different caracteristics are needed this triple Fourier series can be very expensive to evaluate each timestep

Multiwaves schemes:

Garcia et al. (2007),
Alexander and Dunkerton (1999)
Treat the large ensemble of waves but each quite independently from the others and using Lindzen (1981) to evaluate the breaking.

Globally spectral schemes:

Treat the spectra globally, and using analytical integrals of its different parts

Hine (1997),
Manzini and McFarlane (1997)

Warner and McIntyre (2001)

Gravity waves from fronts and convection
2) Globally spectral versus multiwave parameterization schemes

Globally spectral schemes,

Use that the observed GWs vertical (m-)spectra have a quasi-universal shape, with a m^{-3} slope for the $m>m^*$ part of the spectra that correspond to breaking waves

m -slope (conservative propagation)

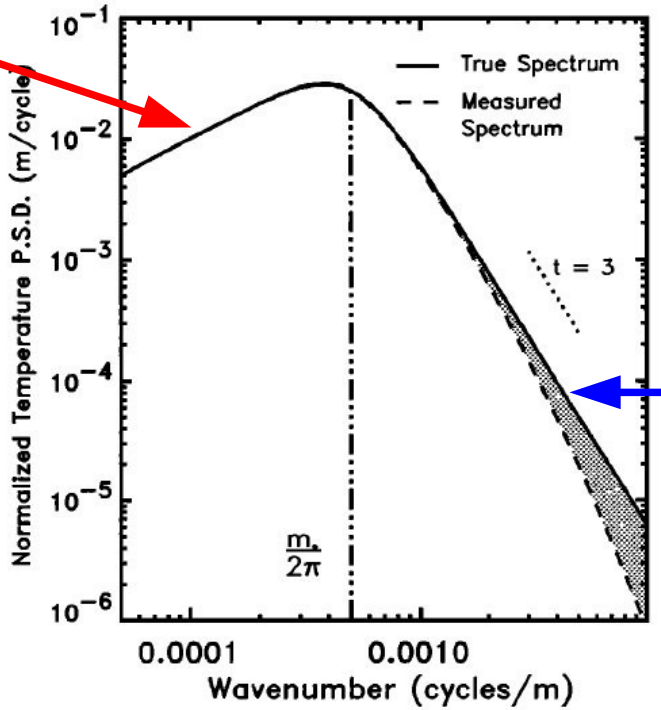

Figure 3. The theoretical distortion of a modified-Desaubies vertical wavenumber power spectrum measured by a radiosonde with temperature sensor response time $\tau = 8$ s and with vertical ascent velocity $V_0 = 5$ m s^{-1}. The shaded region comprises 4% of the total area under the modified-Desaubies spectrum.

m^{-3} -slope (saturated portion)

Modified Desaubie (1976)'s vertical wavenumber spectra (VanZandt and Fritts 1989)

Gravity waves from fronts and convection
2) Globally spectral versus multiwave parameterization schemes

Globally spectral schemes,

Use that the observed GWs vertical (m-)spectra have a quasi-universal shape, with a m^{-3} slope for the $m>m^*$ part of the spectra that correspond to breaking waves

Waves kept m_c

m -slope (conservative propagation)

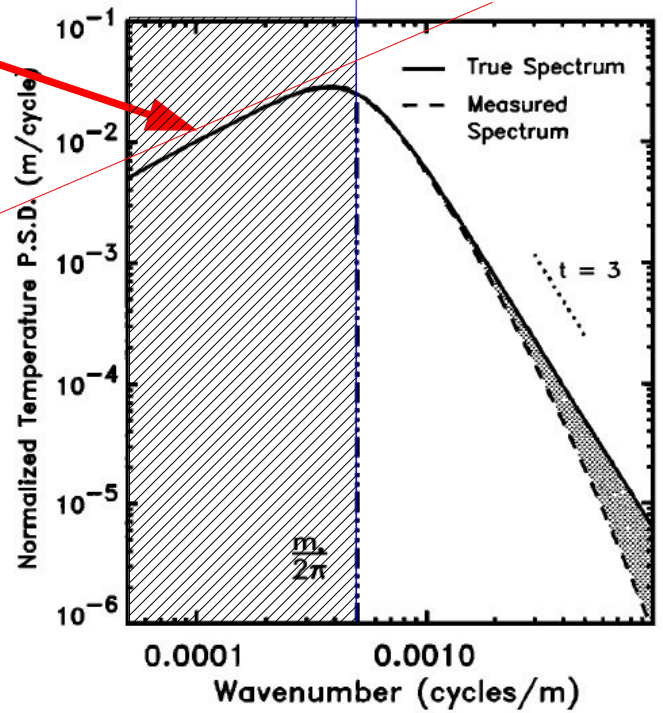

Figure 3. The theoretical distortion of a modified-Desaubies vertical wavenumber power spectrum measured by a radiosonde with temperature sensor response time $\tau = 8$ s and with vertical ascent velocity $V_0 = 5$ m s^{-1}. The shaded region comprises 4% of the total area under the modified-Desaubies spectrum.

Modified Desaubie (1976)'s vertical wavenumber spectra (VanZandt and Fritts 1989)

<u>The Hines (1987)'</u>s scheme consider the m-slope part of the spectra.
It shops the initial spectra more and more with altitude by diagnosing the initial vertical Wave-numbers that are likely to be sufficiently "Doppler spreaded" by the mean-wind **<u>and</u>** by the other waves, to reach a "critical level", by evaluating a cut-off value:

$$m_c = \frac{N_i}{\Phi\,\sigma + V - V_i}$$

Initial BV

Initial Wind

Wind variance due to waves

Wind at level considered

Φ: "fudge factor"

Gravity waves from fronts and convection
2) Globally spectral versus multiwave parameterization schemes

Globally spectral schemes,

Use that the observed GWs vertical (m-)spectra have a quasi-universal shape, with a m^{-3} slope for the $m>m^*$ part of the spectra that correspond to breaking waves

Waves kept ← m_c **Altitude increases**

m -slope (conservative propagation)

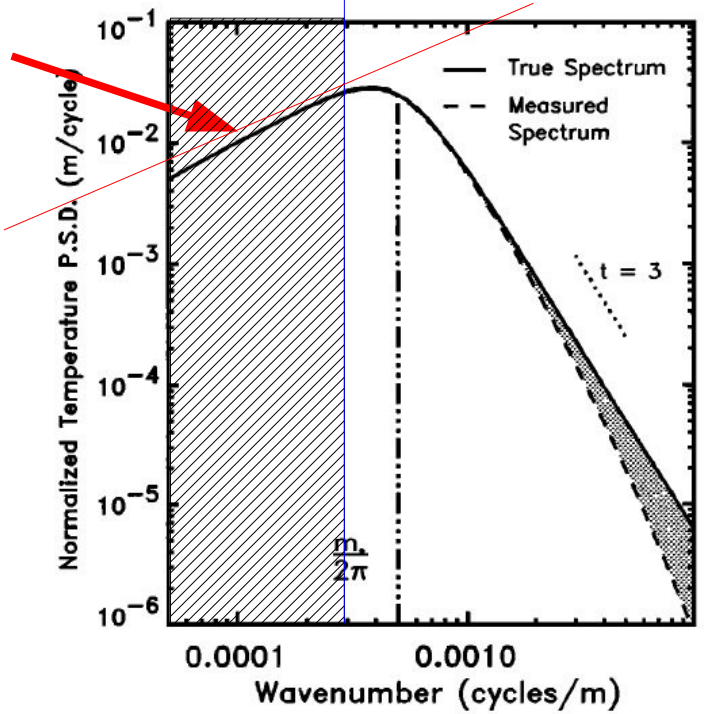

Figure 3. The theoretical distortion of a modified-Desaubies vertical wavenumber power spectrum measured by a radiosonde with temperature sensor response time $\tau = 8$ s and with vertical ascent velocity $V_0 = 5$ m s^{-1}. The shaded region comprises 4% of the total area under the modified-Desaubies spectrum.

Modified Desaubie (1976)'s vertical wavenumber spectra (VanZandt and Fritts 1989)

<u>The Hines (1987)'</u>s scheme consider the m-slope part of the spectra.
It shops the initial spectra more and more with altitude by diagnosing the initial vertical Wave-numbers that are likely to be sufficiently "Doppler spreaded" by the mean-wind **<u>and</u>** by the other waves, to reach a "critical level", by evaluating a cut-off value:

$$m_c = \frac{N_i}{\Phi\,\sigma + V - V_i}$$

N_i ← Initial BV

Initial Wind → V

σ: Wind variance due to waves

V_i: Wind at level considered

Φ: "fudge factor"

Gravity waves from fronts and convection
2) Globally spectral versus multiwave parameterization schemes

Globally spectral schemes,

Use that the observed GWs vertical (m-)spectra have a quasi-universal shape, with a m^{-3} slope for the $m>m^*$ part of the spectra that correspond to breaking waves

Waves kept ← m_c **Altitude increases further**

m -slope (conservative propagation)

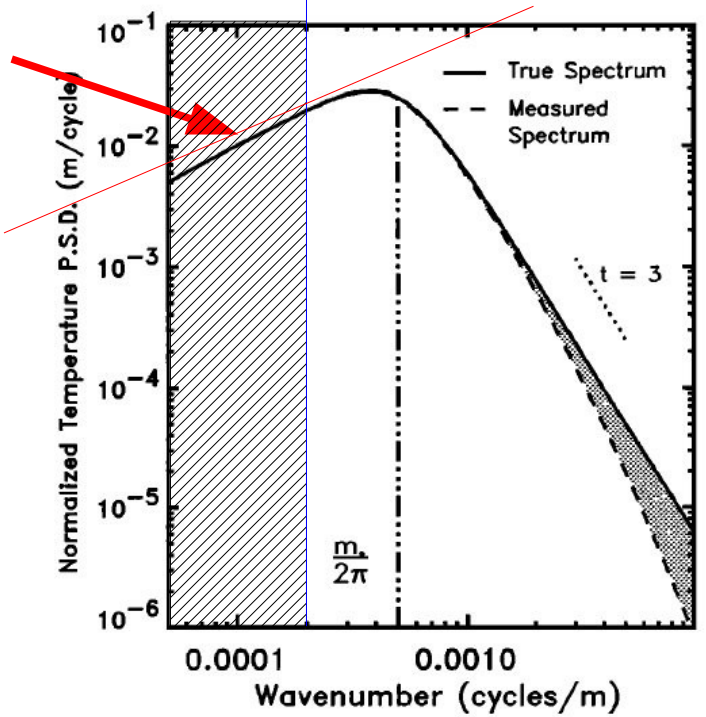

Figure 3. The theoretical distortion of a modified-Desaubies vertical wavenumber power spectrum measured by a radiosonde with temperature sensor response time $\tau = 8$ s and with vertical ascent velocity $V_0 = 5$ m s^{-1}. The shaded region comprises 4% of the total area under the modified-Desaubies spectrum.

Modified Desaubie (1976)'s vertical wavenumber spectra (VanZandt and Fritts 1989)

<u>The Hines (1987)'</u>s scheme consider the m-slope part of the spectra.
It shops the initial spectra more and more with altitude by diagnosing the initial vertical Wave-numbers that are likely to be sufficiently "Doppler spreaded" by the mean-wind **<u>and</u>** by the other waves, to reach a "critical level", by evaluating a cut-off value:

$$m_c = \frac{N_i}{\Phi\,\sigma + V - V_i}$$

N_i ← Initial BV

Initial Wind → V_i

σ: Wind variance due to waves

V: Wind at level considered

Φ: "fudge factor"

Gravity waves from fronts and convection
2) Globally spectral versus multiwave parameterization schemes

Globally spectral schemes,

Use that the observed GWs vertical (m-)spectra have a quasi-universal shape, with a m^{-3} slope for the $m>m^*$ part of the spectra that correspond to breaking waves

Waves kept ← m_c **Altitude increases further again**

m -slope (conservative propagation)

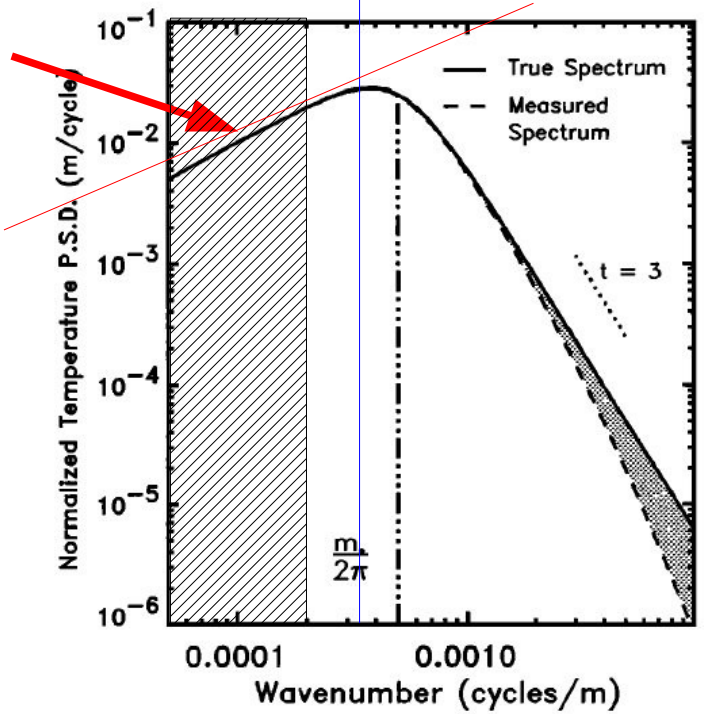

Figure 3. The theoretical distortion of a modified-Desaubies vertical wavenumber power spectrum measured by a radiosonde with temperature sensor response time $\tau = 8$ s and with vertical ascent velocity $V_0 = 5$ m s^{-1}. The shaded region comprises 4% of the total area under the modified-Desaubies spectrum.

Modified Desaubie (1976)'s vertical wavenumber spectra (VanZandt and Fritts 1989)

<u>The Hines (1987)'</u>s scheme consider the m-slope part of the spectra.
It shops the initial spectra more and more with altitude by diagnosing the initial vertical Wave-numbers that are likely to be sufficiently "Doppler spreaded" by the mean-wind **<u>and</u>** by the other waves, to reach a "critical level", by evaluating a cut-off value:

$$m_c = \frac{N_i}{\Phi\,\sigma + V - V_i}$$

N_i ← Initial BV

Initial Wind → V_i

σ: Wind variance due to waves

V: Wind at level considered

Φ: "fudge factor"

Gravity waves from fronts and convection
3) Stochastic GWs scheme, application to convection

Classical arguments: see Palmer et al. 2005, Shutts and Palmer 2007, for the GWs: Piani et al. (2005, globally spectral scheme) and Eckeman (2011, multiwaves scheme)

1) The spatial steps Δx and Δy of the unresolved waves is not a well defined concept (even though they are probably related to the model gridscales δx δy). The time scale of the GWs life cycle Δt is certainly larger than the time step (δt) of the model, and is also not well defined.

2) The mesoscale dynamics producing GWs is not well predictable (for the mountain gravity waves see Doyle et al. MWR 11).

These calls for an extension of the concept of triple Fourier series, which is at the basis of the subgrid scale waves parameterization to that of stochastic series:

$$w' = \sum_{n=1}^{\infty} C_n w'_n \qquad \text{where} \qquad \sum_{n=1}^{\infty} C_n^2 = 1$$

The C'_ns generalised the intermittency coefficients of Alexander and Dunkerton (1995), and used in Beres et al. (2005).

Gravity waves from fronts and convection
3) Stochastic GWs scheme, application to convection

For the w'_n we use linear WKB theory of hydrostatic GWs, and treat the breaking as if each w'_n was doing the entire wave field (using Lindzen (1982)'s criteria for instance):

$$w'_n = \Re\left\{ \hat{w}_n(z)\, e^{z/2\mathrm{H}}\, e^{i(k_n x + l_n y - \omega_n t)} \right\} \qquad \hat{w}_n, k_n, l_n, \omega_n \quad \text{chosen randomly}$$

WKB passage from one level to the next with a small dissipation (Eliasen Palm flux):

$$\vec{F}(z+dz) = \frac{\vec{k}}{|\vec{k}|}\, sign(\Omega) \left(\frac{1 + sign(\Omega(z+\delta z)\cdot\Omega(z))}{2} \right) Min\left(|\vec{F}(z)|\, e^{-2\frac{\nu m^3}{\Omega}\delta z},\ \rho_r \frac{|\Omega^3|}{2N} e^{-(z+\delta z)/H} S_c^2 \frac{k^{*2}}{|\vec{k}^4|} \right)$$

Critical level

Eliasen-Palm theorem with dissipation

Breaking

S_c, k^*: Tunable parameters

$$m = \frac{N|\vec{k}|}{\Omega}$$ Vertical wavenumber

$$\Omega = \omega - \vec{k}\cdot\vec{u}$$ Intrinsic frequency

Few waves (say M=8) are launched at each physical time step (δt=30mn), but their effect is redistributed over a longer time scale (Δt=1day), via an AR-1 protocole:

$$\left(\frac{\partial \vec{u}}{\partial t}\right)_{GWs}^{t+\delta t} = \frac{\Delta t - \delta t}{\Delta t}\left(\frac{\partial \vec{u}}{\partial t}\right)_{GWs}^{t} + \frac{\delta t}{M \Delta t} \sum_{n'=1}^{M} \frac{1}{\rho} \frac{\partial \vec{F}_n^z}{\partial z}$$

Gravity waves from fronts and convection
3) Stochastic GWs scheme, application to convection

$$P'_r = \sum_{n=1}^{\infty} C_n P_n' \quad \text{where} \quad P_n' = \Re\left[\hat{P}_n e^{i(\vec{k}_n \cdot \vec{x} - \omega_n t)}\right] \qquad \text{taking} \qquad \left|\hat{P}_n\right| = P_r$$

The subgrid scale standard deviation of the precipitation equals the gridscale mean

Distributing the related diabatic forcing over a depth Δz it is quite easy to place the forcing in the right hand side of a "wave" equation:

$$\rho c_p \left(\frac{DT'}{dt} + \frac{DT_0}{dz} w' \right) = L_w P' \frac{e^{-z^2/\Delta z^2}}{\Delta z} \quad \rightarrow \quad \frac{\Omega^2}{k^2} \hat{w}_{zz} + N^2 \hat{w} = \frac{R L_w}{\rho H c_p} \hat{P} \frac{e^{-z^2/\Delta z^2}}{\Delta z}$$

EP-flux at the launch level:

$$\vec{F}_{nl} = \rho_r \frac{\vec{k}_n}{\left|\vec{k}_n\right|} \frac{\left|\vec{k}_n\right|^2 e^{-m_n^2 \Delta z^2}}{N \Omega_n^3} G_{uw} \left(\frac{R L_W}{\rho_r H c_p} \right)^2 P_r^2$$

New tuning parameter (could be a random number)

k_n, l_n, ω_n Are still chosen randomly $m_n = \frac{N\left|\vec{k}_n\right|}{\Omega_n}, \Omega_n = \omega_n - \vec{k}_n \cdot \vec{U}$

Gravity waves from fronts and convection
3) Stochastic GWs scheme, application to convection

Offline tests with ERAI and GPCP

G_{uw}=2.4, S_c=0.25,
k*=0.02km^{-1},
m=1kg/m/s
Dt=1day and M=8
Dz=1km (source depth~5km)

The CGWs stress is now well distributed along where there is strong precipitations

It is stronger on average in the tropical regions, but quite significant in the midlatitudes.

The zonal mean stress comes from very large values issued from quite few regions.

Precipitations and surface stresses averaged over 1week (1-7 January 2000) **Results for GPCP data and ERAI**

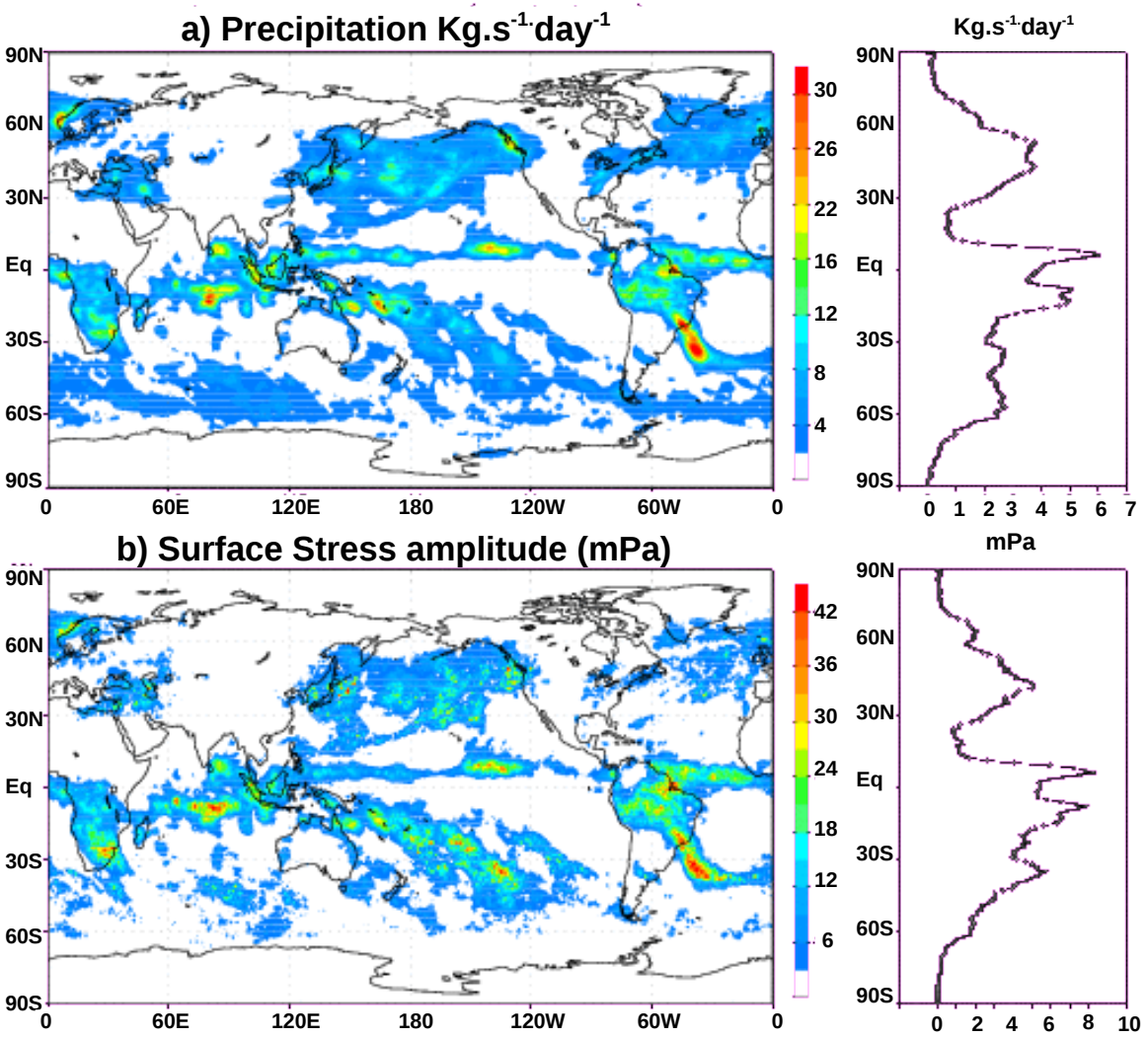

Gravity waves from fronts and convection
3) Stochastic GWs scheme, application to convection

Offline tests with ERAI and GPCP

Benefit of having few large GWs rather than a large ensemble of small ones:

Real precip. Stress amplitude (CI=2mPa)

Uniformized precip. Stress amplitude (CI=2mPa)

CGWs stress

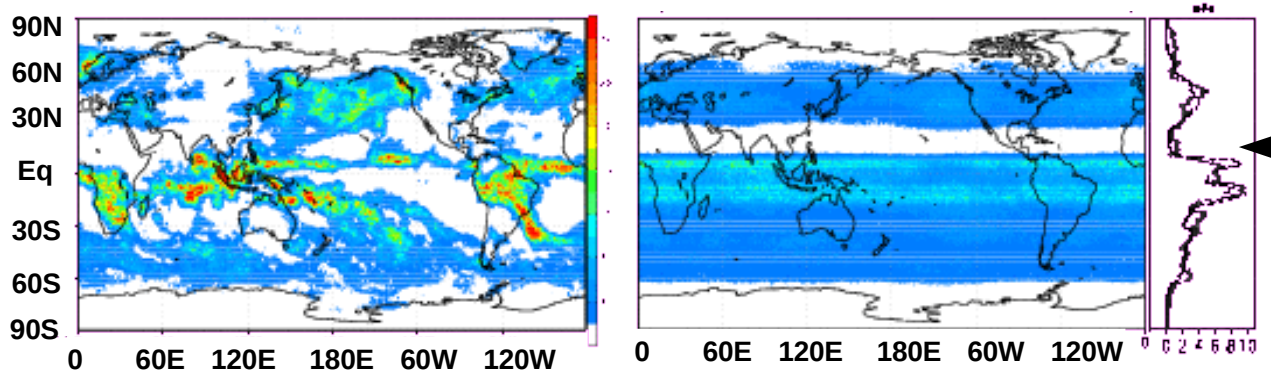

Same zonal mean stress

Real precip. du/dt *e(-z/2H), CI= 0.1 m/s/d

Uniformized precip. du/dt *e(-z/2H), CI= 0.1 m/s/d

CGWs drag

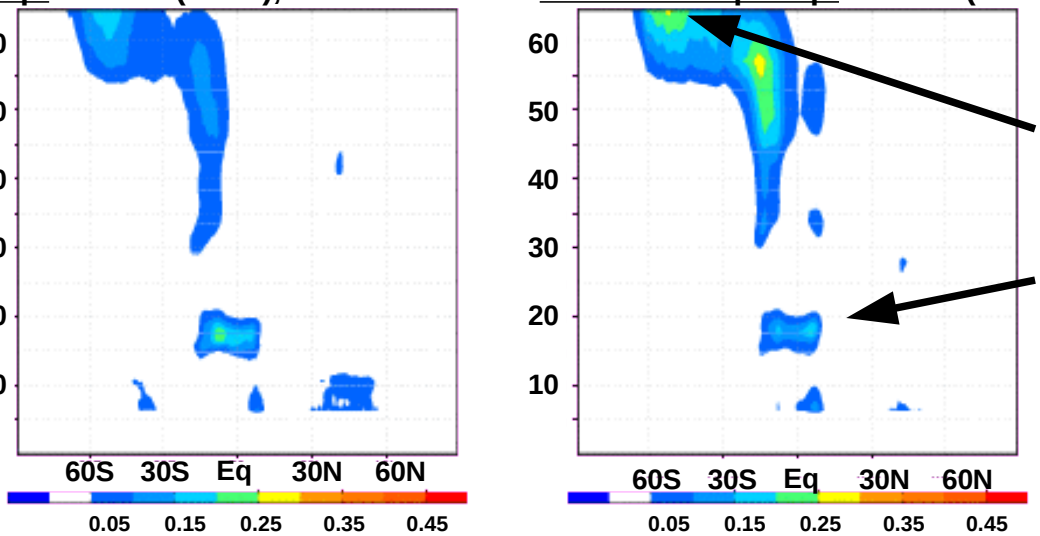

More drag near and above stratopause

Slightly less drag in the QBO region

Lott and Guez, JGR 2013

Gravity waves from fronts and convection
3) Stochastic GWs scheme, application to convection

Online results with LMDz

LMDz version with 80 levels, dz<1km
In the stratosphere

QBO of irregular
period with mean
around 26month,

20% too small amplitude

Westerly phase lacks of connection with the stratopause SAO

a) LMDz with convective GWs **LMDz+CGWs**

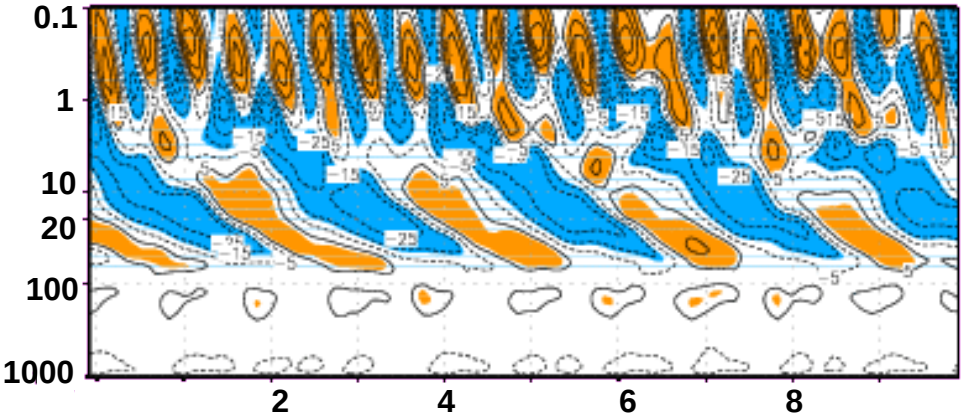

b) MERRA

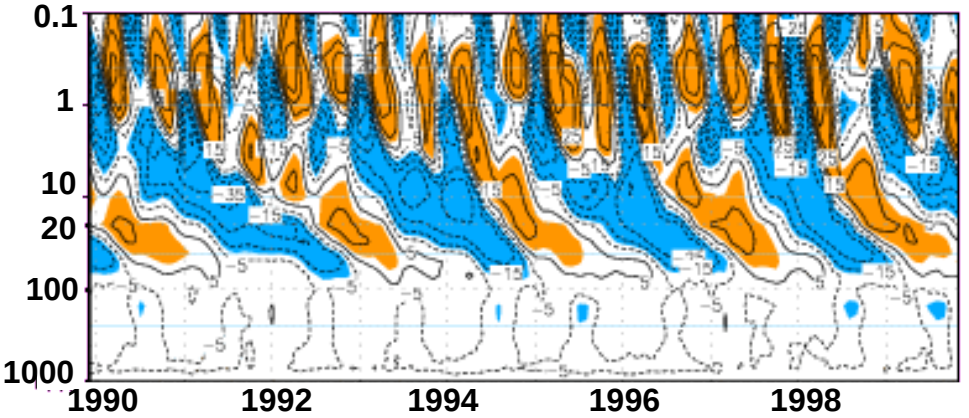

Lott and Guez, JGR13

Gravity waves from fronts and convection
3) Stochastic GWs scheme, application to convection

Online results with LMDz

Histogram of QBO periods

Relatively good spread of the periods taking into account that it is a forced simulation with climatological SST (no ENSO)

Periods related to the annual cycle (multiples of 6 months) are not favoured probably related to the weak relations with the SAO

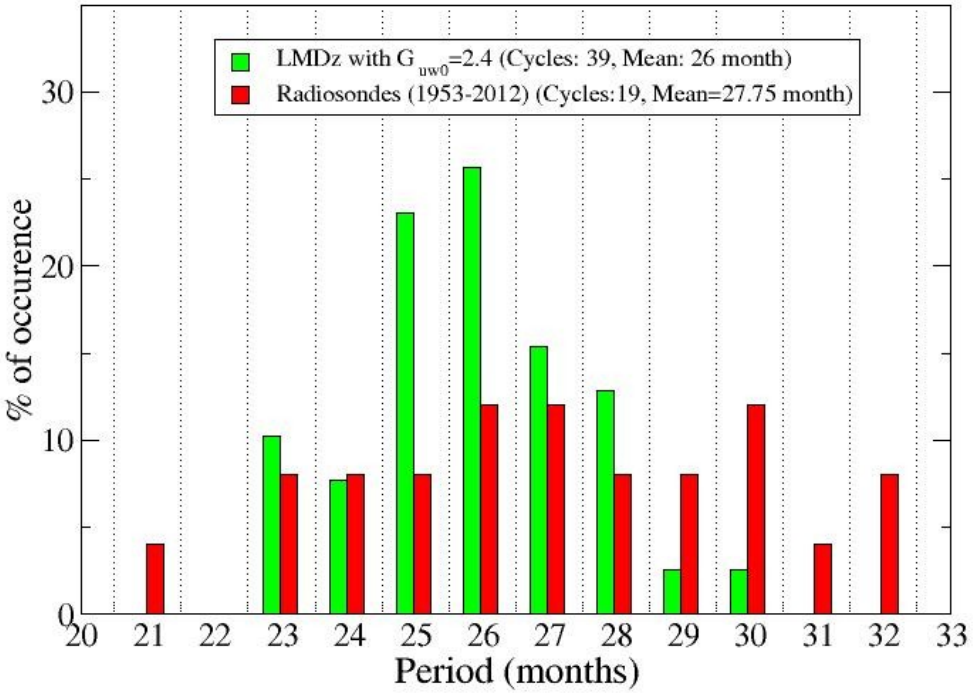

Lott and Guez, JGR13

Gravity waves from fronts and convection
3) Stochastic GWs scheme, application to convection

SAO:

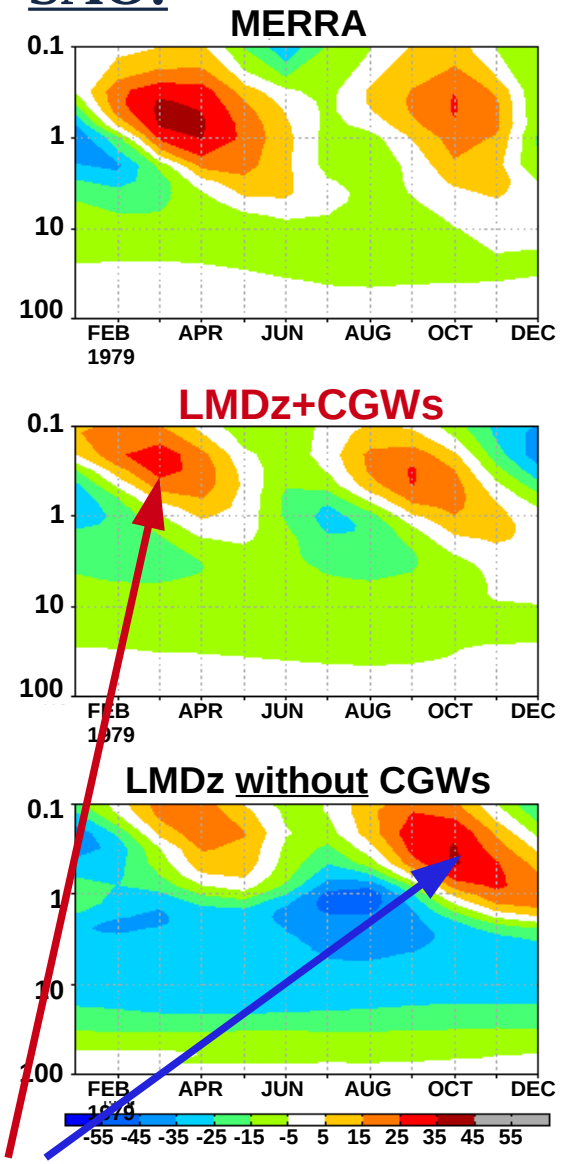

No negative impacts on other climatological aspects of the model

January zonal mean zonal wind

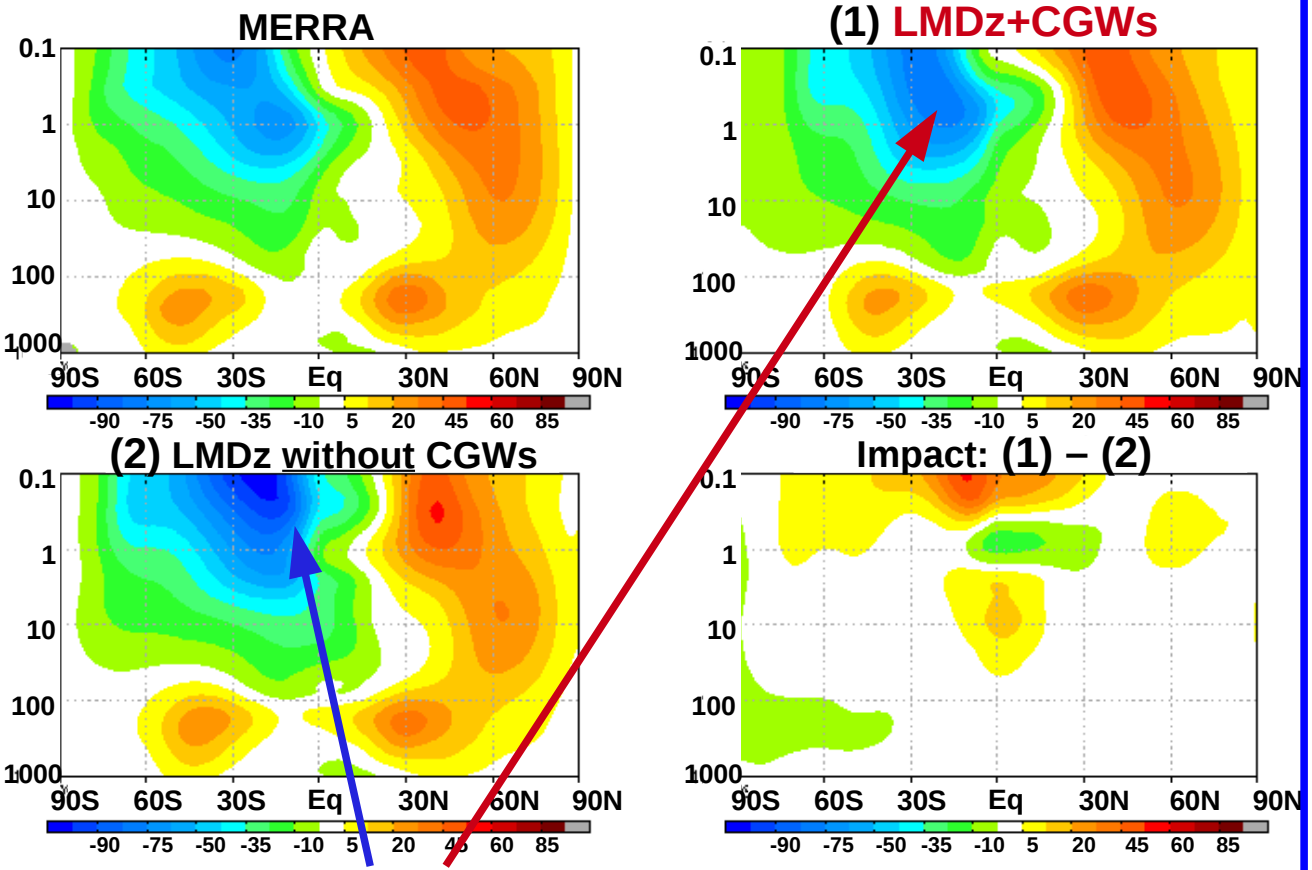

CGWs improve the phase at the stratopause

CGWs reduce easterly biases in the subtropics summer mesosphere

Gravity waves from fronts and convection
3) Stochastic GWs scheme, application to convection

Composite of Rossby-gravity waves with s=4-8
Temp (CI=0.1K) and Wind at 50hPa & lag = 0day

Equatorial waves:

Remember also that when you start to have positive zonal winds, **the planetary scale Yanai wave is much improved**

(the composite method is described in Lott et al. 2009)

Zero longitude line arbitrary

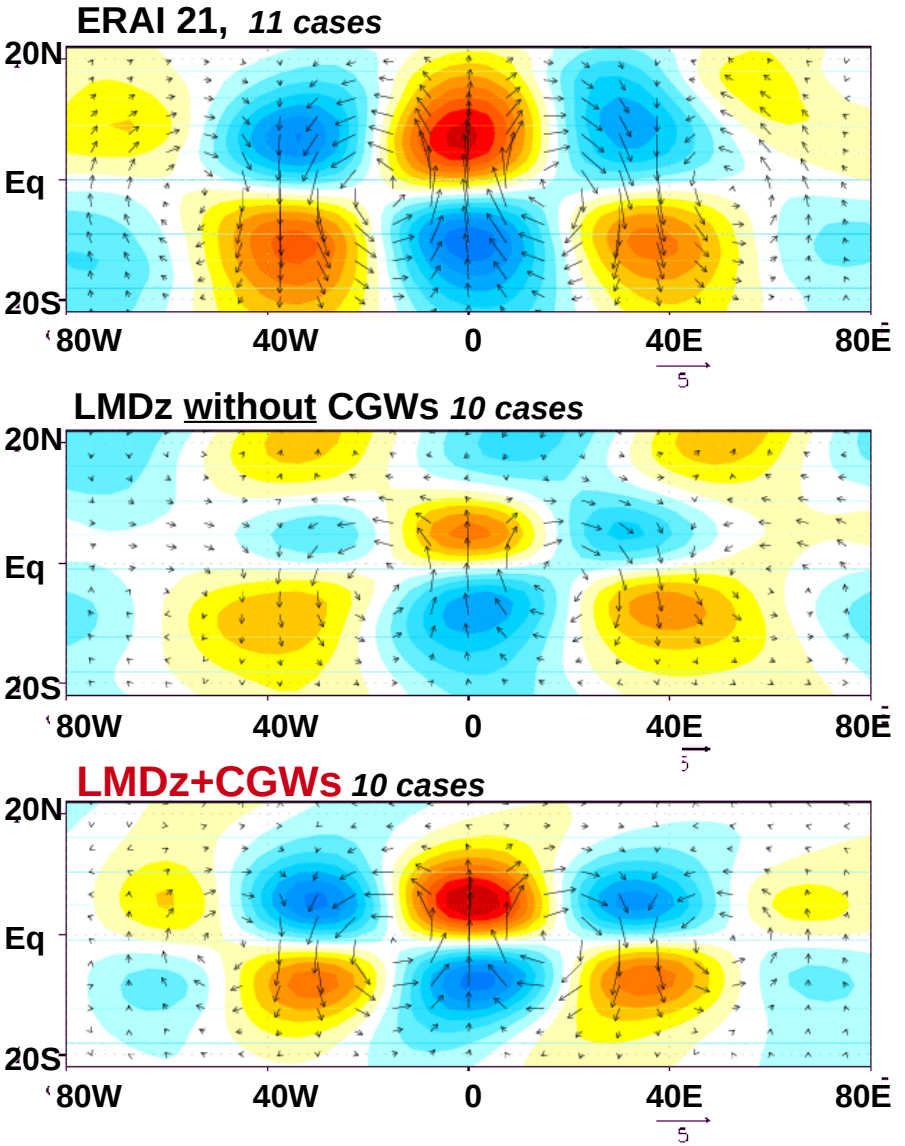

Lott et al. 2012 GRL

Gravity waves from fronts and convection
3) Stochastic GWs scheme, application to convection

Equatorial waves:

Remember that
when you have
No QBO, the zonal winds are
negative, , **the**
planetary scale Kelvin wave
Becomes to strong

(the composite method is described in Lott et al. 2009)

Zero longitude line arbitrary

Lott et al. 2012 GRL

Composite of Kelvin waves with s=1-6
Temp (CI=0.5K) and Wind at 50hPa & lag = 0day

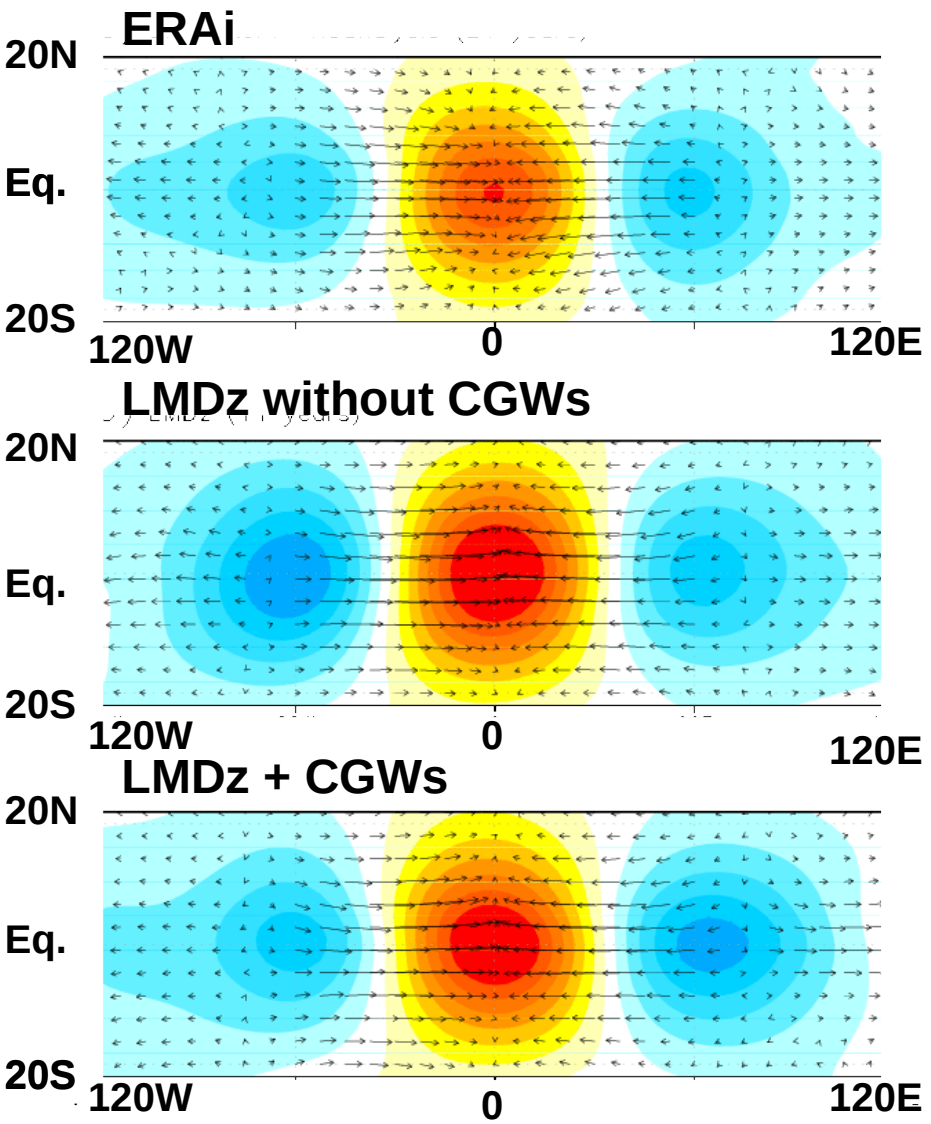

Gravity waves from fronts and convection
4) GWs from front via a “smoking gun” approach

For waves from front, the situation is more complex because it is the large scale flow itself that produces a dynamical “ageostrophic” forcing. In the response to this forcing it is still an issue to determine the part that is constituted of GWs from the balanced part.

Some nevertheless uses this frontogenesis function as an indicator. For instance in Richter et al.~(2010), it is said that when

$$F = -\left(\frac{1}{a\cos\varphi}\frac{\partial\theta}{\partial\lambda}\right)^2\left(\frac{1}{a\cos\varphi}\frac{\partial u}{\partial\lambda} - \frac{v\tan\varphi}{a}\right) - \left(\frac{1}{a}\frac{\partial\theta}{\partial\varphi}\right)^2\left(\frac{1}{a}\frac{\partial v}{\partial\varphi}\right) - \left(\frac{1}{a\cos\varphi}\frac{\partial\theta}{\partial\lambda}\right)\left(\frac{1}{a}\frac{\partial\theta}{\partial\varphi}\right)\left(\frac{1}{a\cos\varphi}\frac{\partial v}{\partial\lambda} + \frac{1}{a}\frac{\partial u}{\partial\varphi} + \frac{u\tan\varphi}{a}\right)$$

Exceeds 0.045 (K^2 $(100km)^{-2}$ h^{-1}), GWF=1.5 mPa!

Justification for being so vague :
“the relation between frontal characteristics and wave amplitude have not been established to date”

Gravity waves from fronts and convection
4) GWs from front via a “smoking gun” approach

Simulations to support these parameterizations:

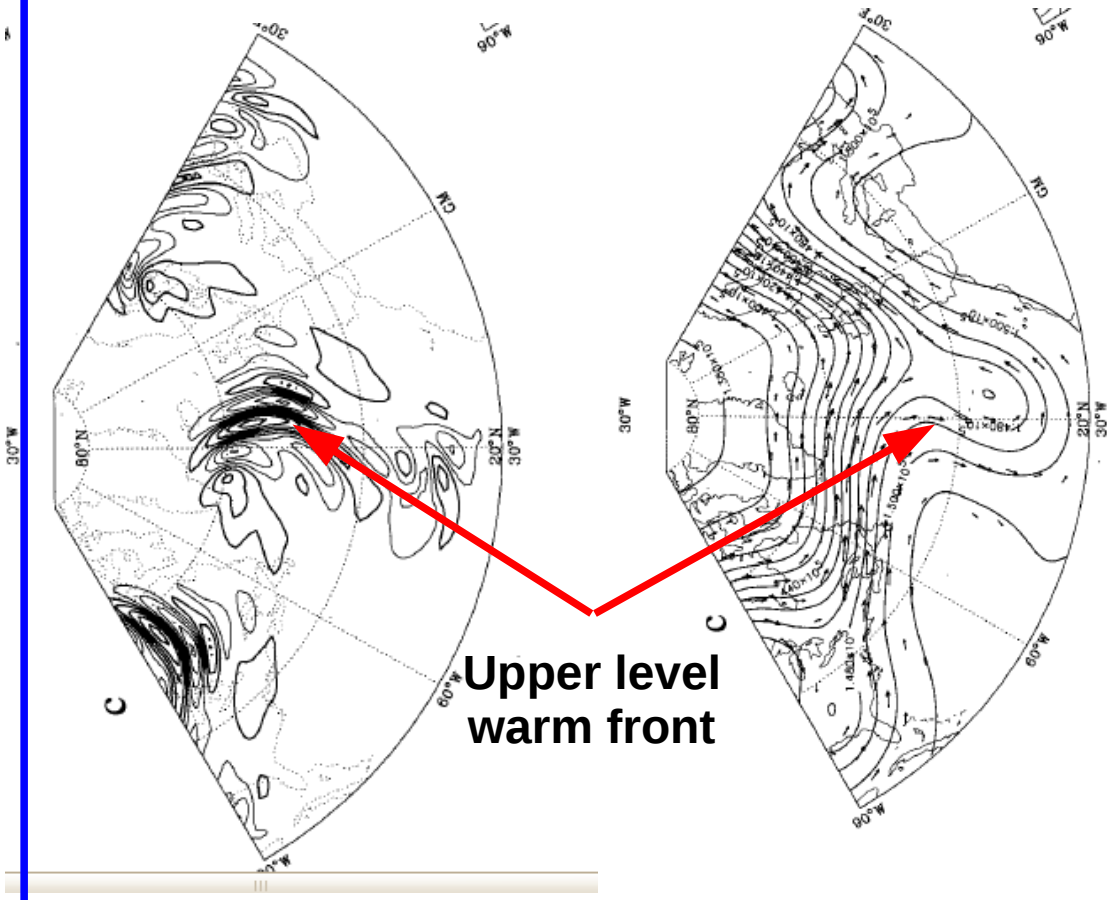

O'Sullivan and Dunkerton (1995)

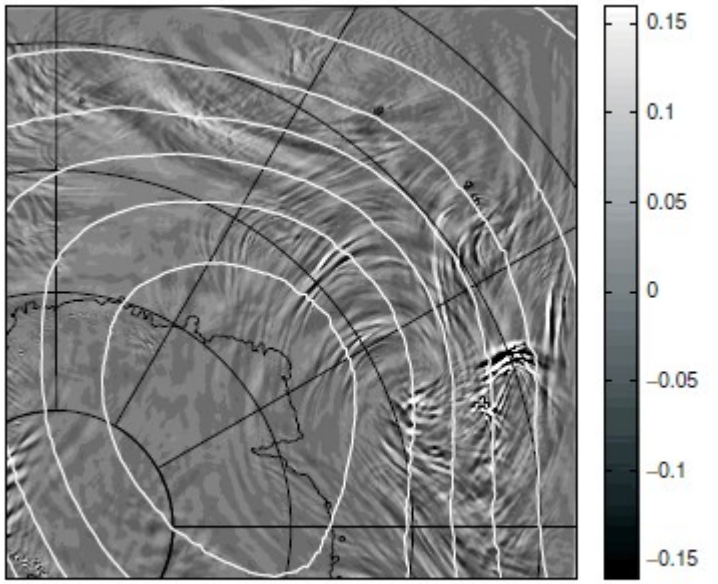

Figure 16. As Figure 2(b), but from a simulation with doubled horizontal resolution ($\Delta x = 10$ km).

Results confirmed by much higher resolution simulations

Plougonven Hertzog and Guez (2012)

Gravity waves from fronts and convection
4) GWs from front via a “smoking gun” approach

2D simulations of frontogenesis (Reeder and Griffiths 1995)

Initial Conditions:
Transverse wind and potential T

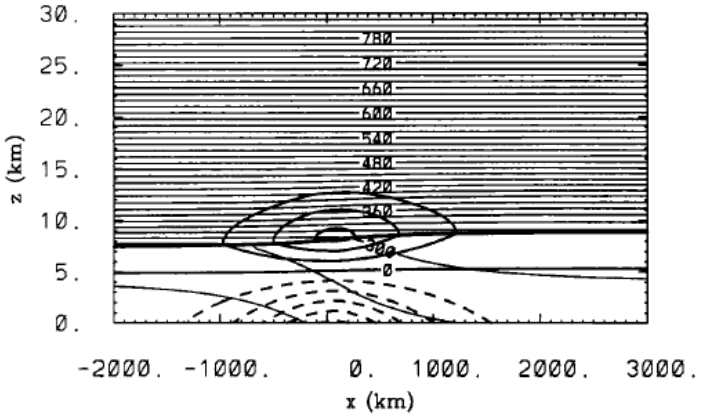

There is also a background along wind shear

The waves are emitted from the front, a place characterised by pronounced potential vorticity anomalies.

Formation of the upper level front

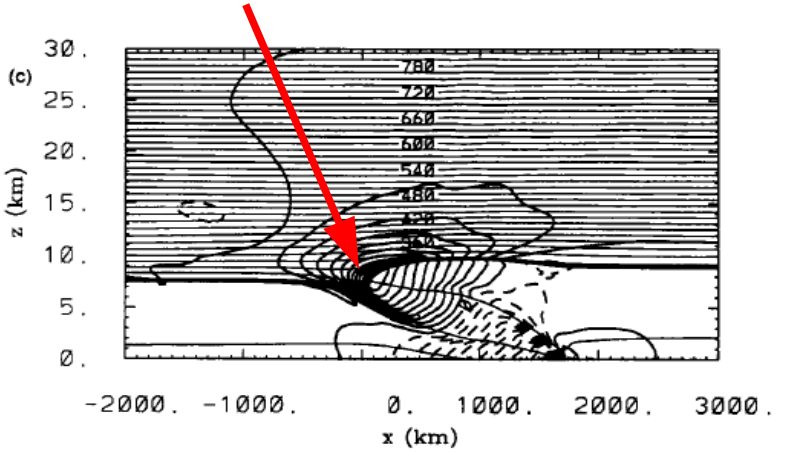

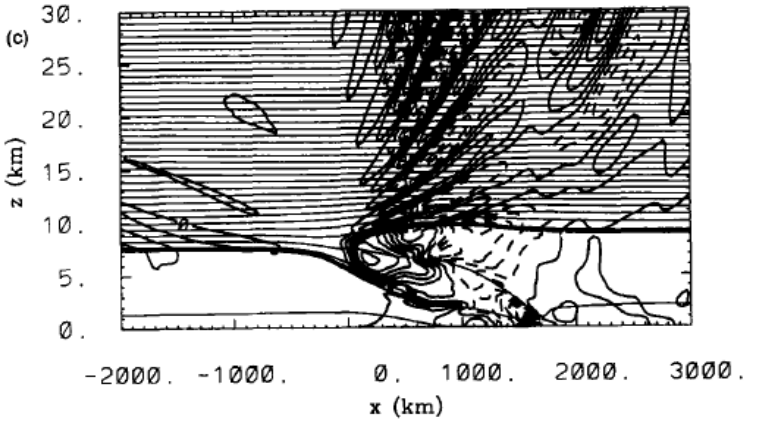

Gravity waves from fronts and convection
4) GWs from front via a “smoking gun” approach

All these processes are somehow related to the well known “Geostrophic Adjustment” Problem.

In the “classical adjustment” an initial unbalanced flow radiates GWs as it returns to a balanced situation. In this case, the initial imbalance is the ultimate source of the GWs: the problem is to know what causes this imbalance (Lott, JAS 2003)

«Spontaneous adjustment» where a well-balanced flow radiates GWs in the course of its evolution. Here the adjustment itself is the GWs source.

In the two cases, there is at the place of largest emission a pronounced PV anomaly, either it is present because the initial conditions are highly perturbed, or it is produced internally

But we know that PV anomalies can spontaneously emit Gravity Waves, and we have exact quantitative estimate of this emission (Lott et al., 2010, 12012). So we can use the PV anomalies themselves as predictors of the GWs emission.

Gravity waves from fronts and convection
4) GWs from front via a "smoking gun" approach

General setup: A 3D (x,y,z) PV anomaly advected in a rotating (*f* =cte), stratified (BV freq ***N*=cte**) shear flow (vertical shear **Λ=cte**).

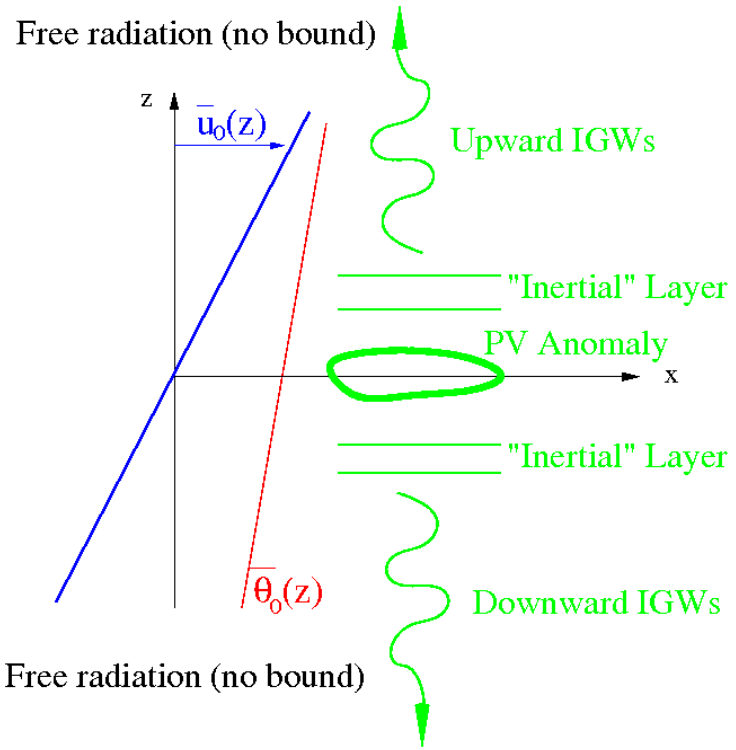

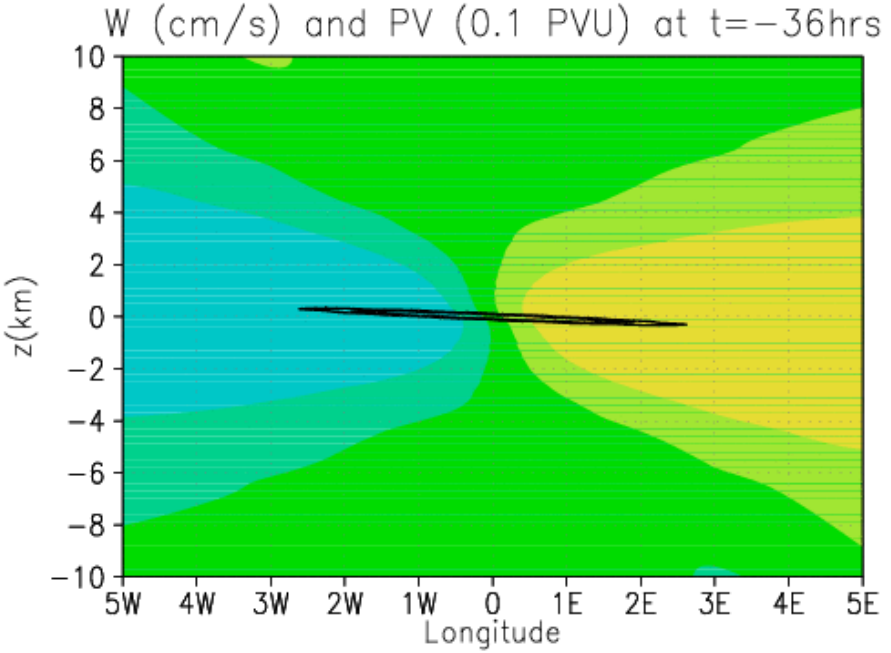

For the 2D results: *Lott, Plougonven and Vanneste, JAS 2010*.

Gravity waves from fronts and convection
4) GWs from front via a "smoking gun" approach

General setup: A 3D (x,y,z) PV anomaly advected in a rotating (*f* =cte), stratified (BV freq ***N*=cte**) shear flow (vertical shear **Λ=cte**).

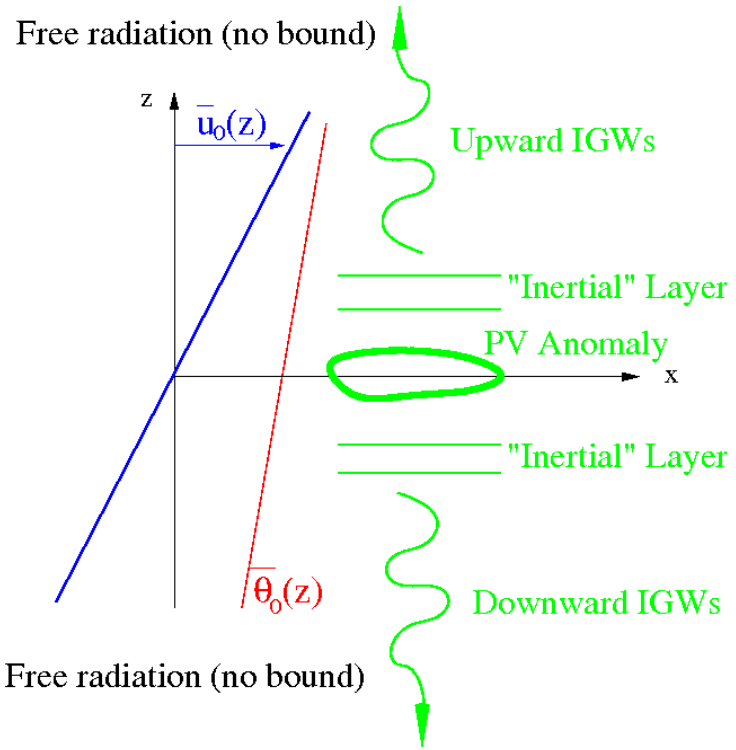

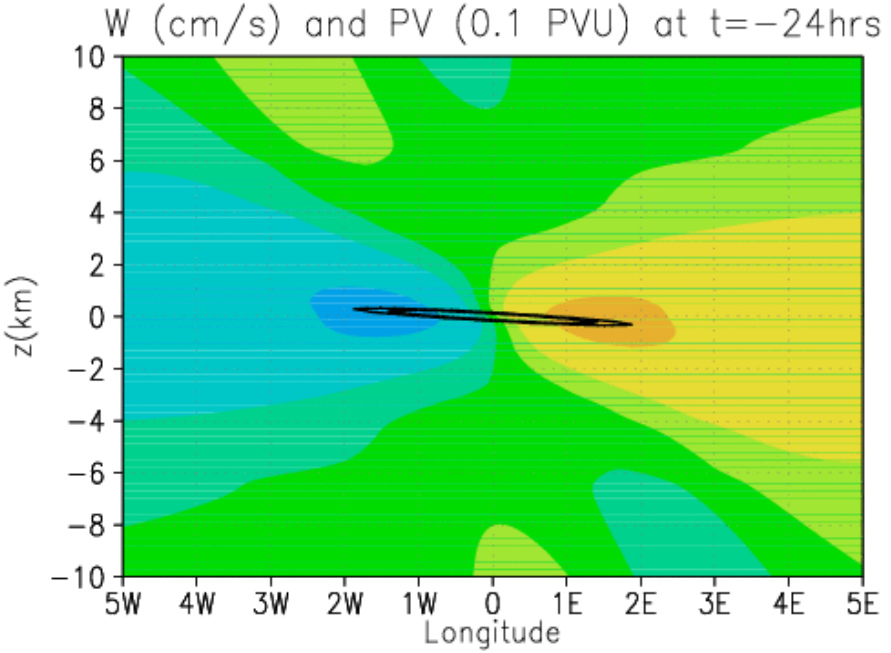

For the 2D results: *Lott, Plougonven and Vanneste, JAS 2010*.

Gravity waves from fronts and convection
4) GWs from front via a "smoking gun" approach

General setup: A 3D (x,y,z) PV anomaly advected in a rotating (*f* =cte), stratified (BV freq ***N*=cte**) shear flow (vertical shear **Λ=cte**).

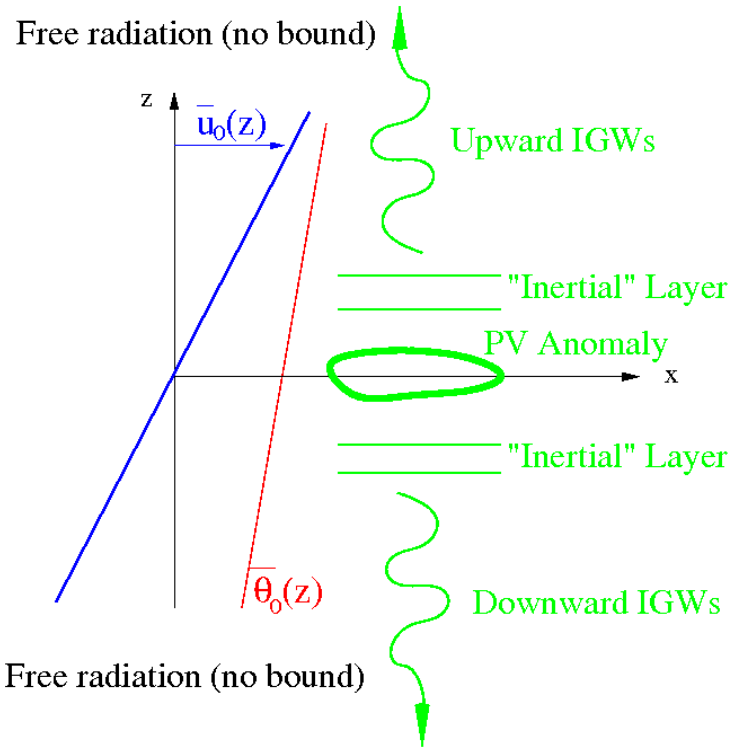

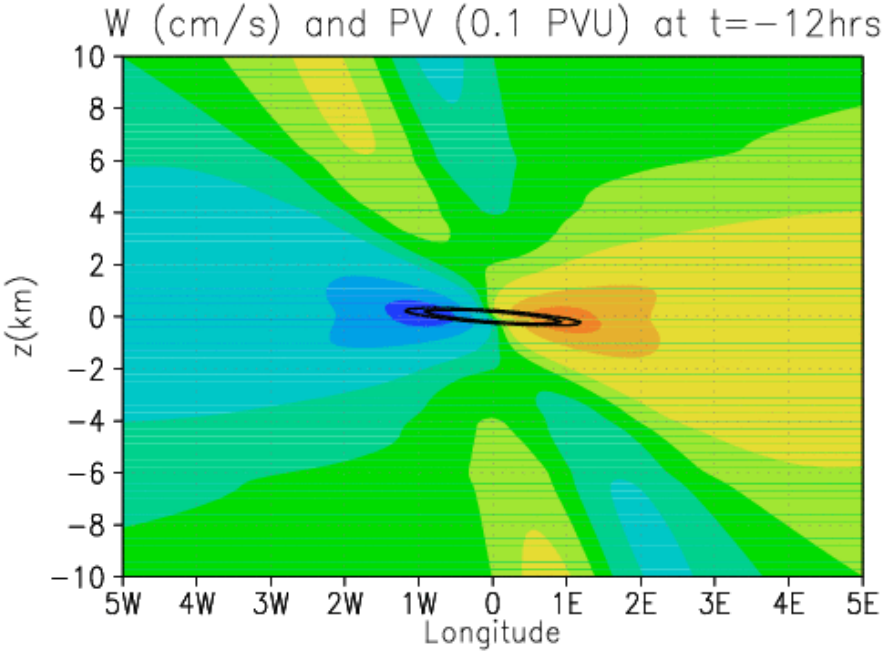

For the 2D results: *Lott, Plougonven and Vanneste, JAS 2010*.

Gravity waves from fronts and convection
4) GWs from front via a "smoking gun" approach

General setup: A 3D (x,y,z) PV anomaly advected in a rotating (*f* =cte), stratified (BV freq ***N*=cte**) shear flow (vertical shear **Λ=cte**).

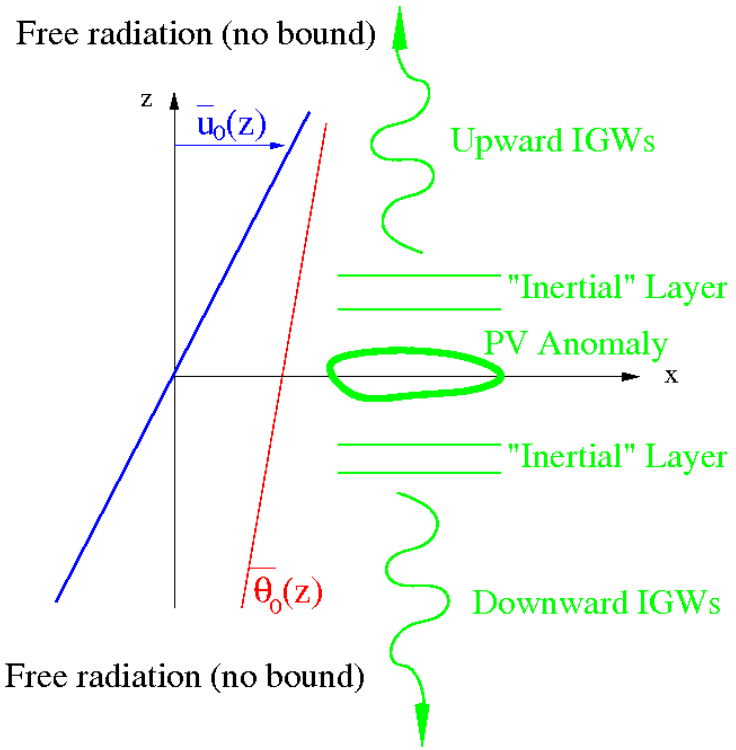

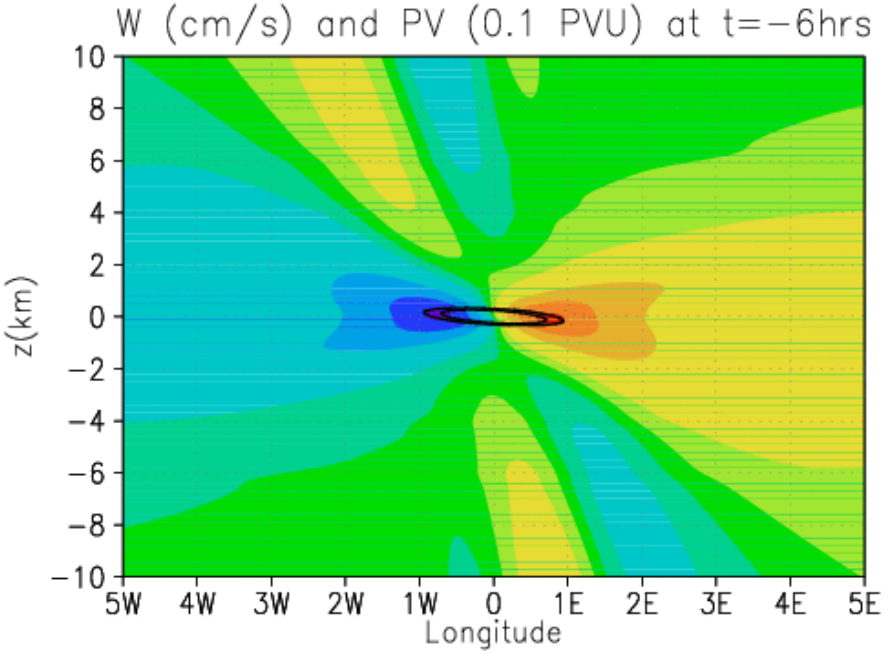

For the 2D results: *Lott, Plougonven and Vanneste, JAS 2010*.

Gravity waves from fronts and convection
4) GWs from front via a "smoking gun" approach

General setup: A 3D (x,y,z) PV anomaly advected in a rotating (*f* =cte), stratified (BV freq ***N*=cte**) shear flow (vertical shear **Λ=cte**).

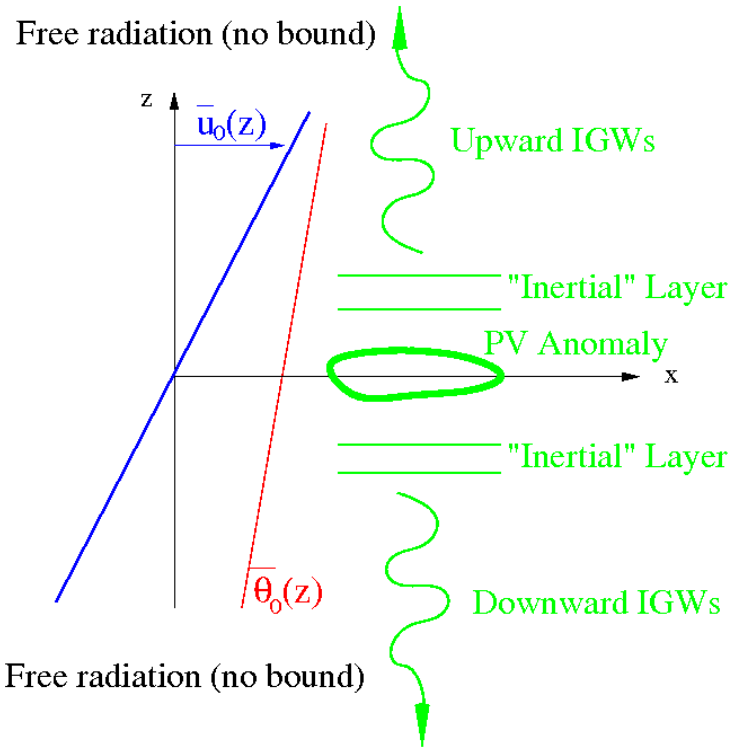

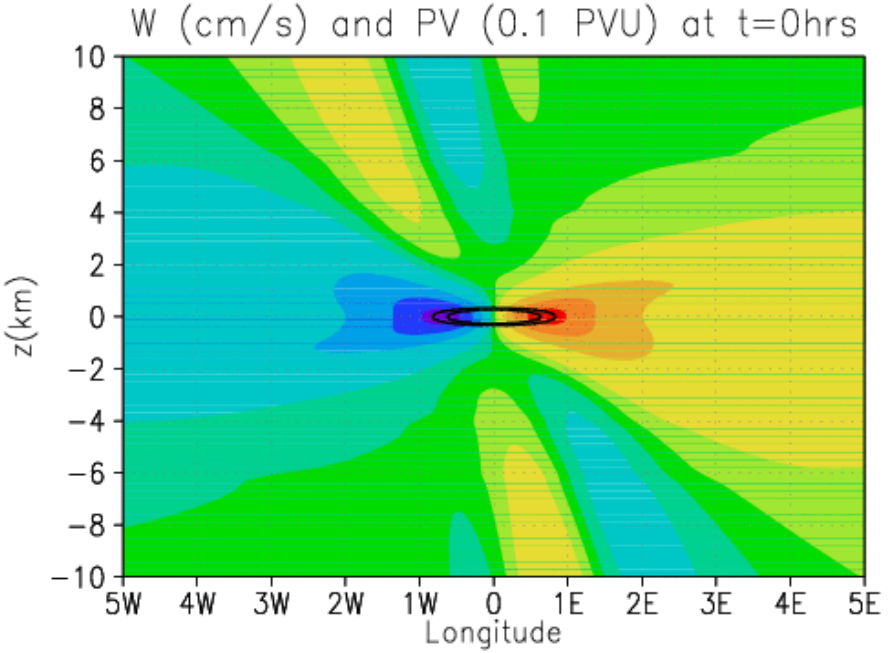

For the 2D results: *Lott, Plougonven and Vanneste, JAS 2010*.

Gravity waves from fronts and convection
4) GWs from front via a "smoking gun" approach

General setup: A 3D (x,y,z) PV anomaly advected in a rotating (*f* =cte), stratified (BV freq ***N*=cte**) shear flow (vertical shear **Λ=cte**).

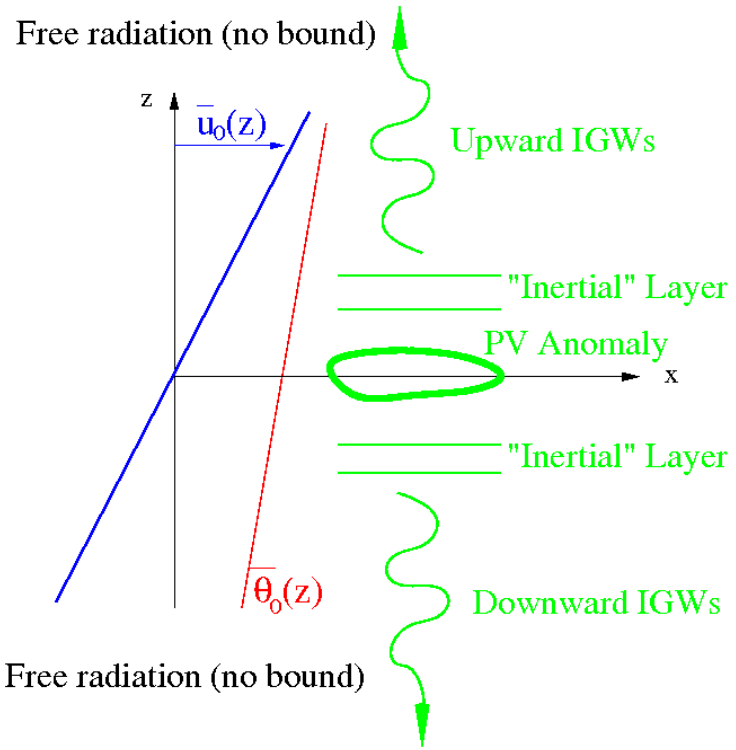

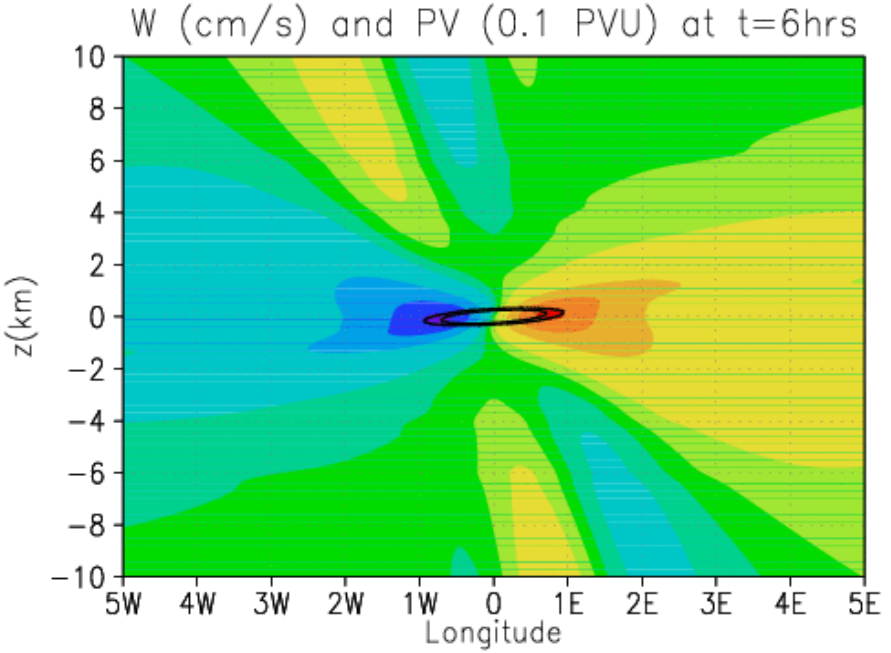

For the 2D results: *Lott, Plougonven and Vanneste, JAS 2010*.

Gravity waves from fronts and convection
4) GWs from front via a "smoking gun" approach

General setup: A 3D (x,y,z) PV anomaly advected in a rotating (*f* =cte), stratified (BV freq ***N*=cte**) shear flow (vertical shear **Λ=cte**).

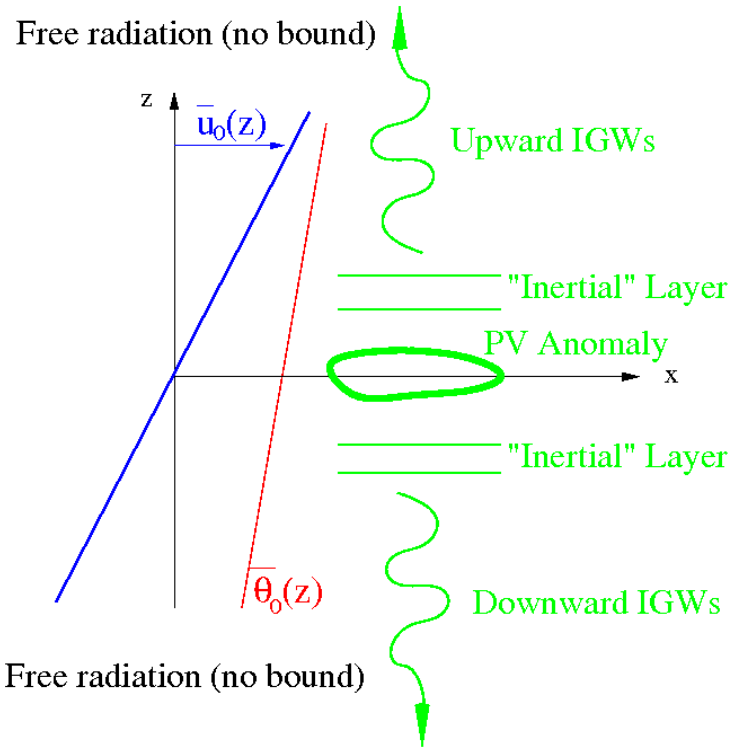

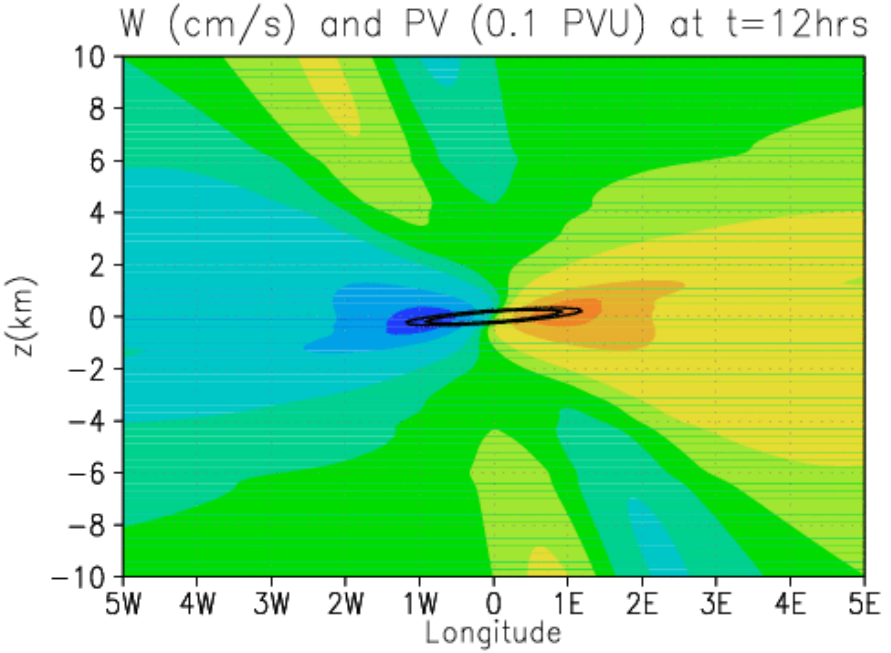

For the 2D results: *Lott, Plougonven and Vanneste, JAS 2010*.

Gravity waves from fronts and convection
4) GWs from front via a "smoking gun" approach

General setup: A 3D (x,y,z) PV anomaly advected in a rotating (*f* =cte), stratified (BV freq ***N*=cte**) shear flow (vertical shear **Λ=cte**).

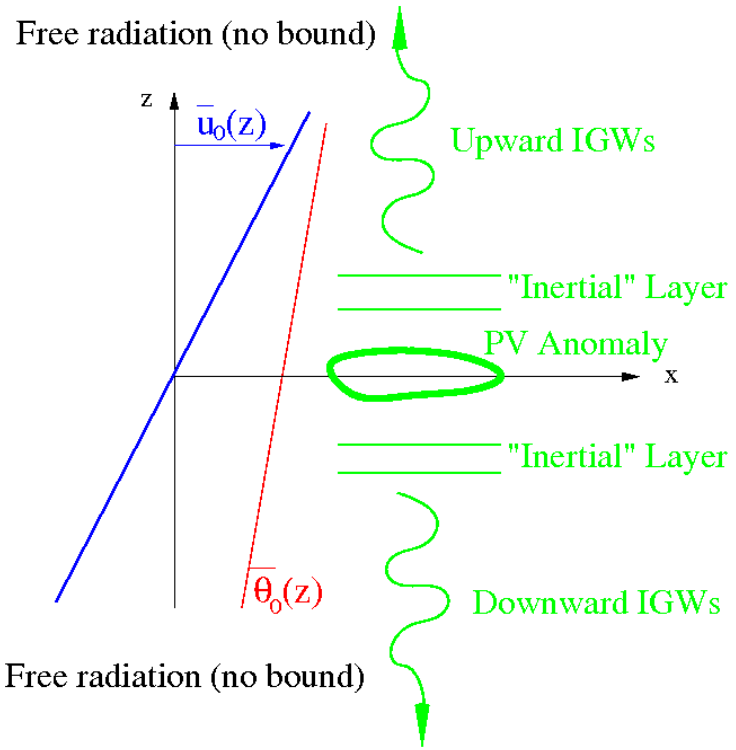

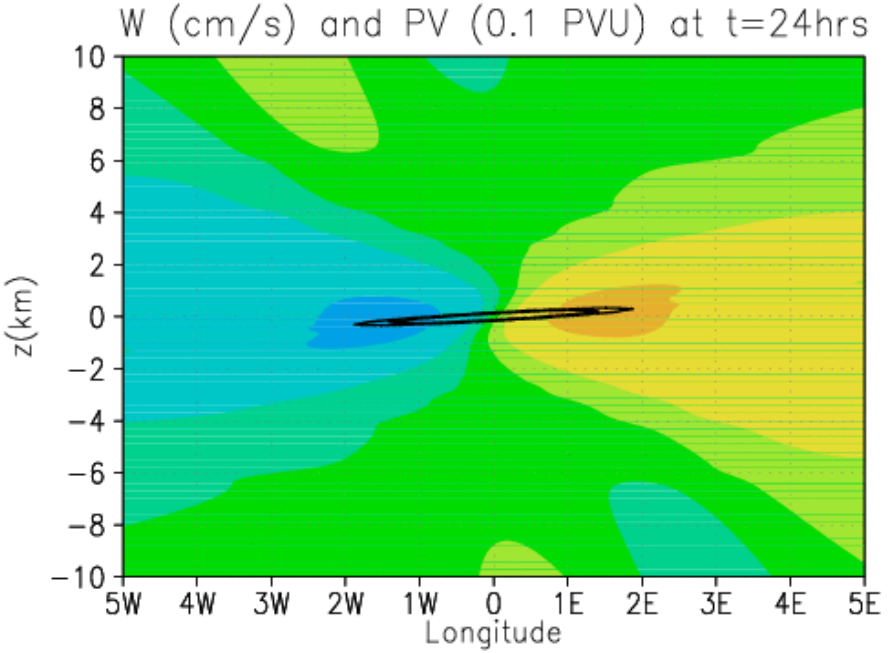

For the 2D results: *Lott, Plougonven and Vanneste, JAS 2010*.

Gravity waves from fronts and convection
4) GWs from front via a "smoking gun" approach

General setup: A 3D (x,y,z) PV anomaly advected in a rotating (*f* =cte), stratified (BV freq ***N*=cte**) shear flow (vertical shear **Λ=cte**).

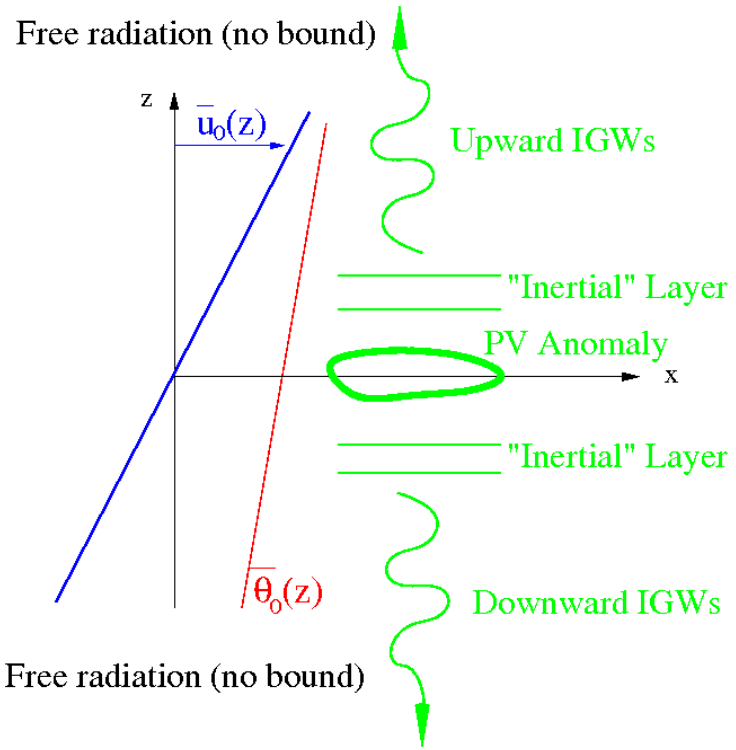

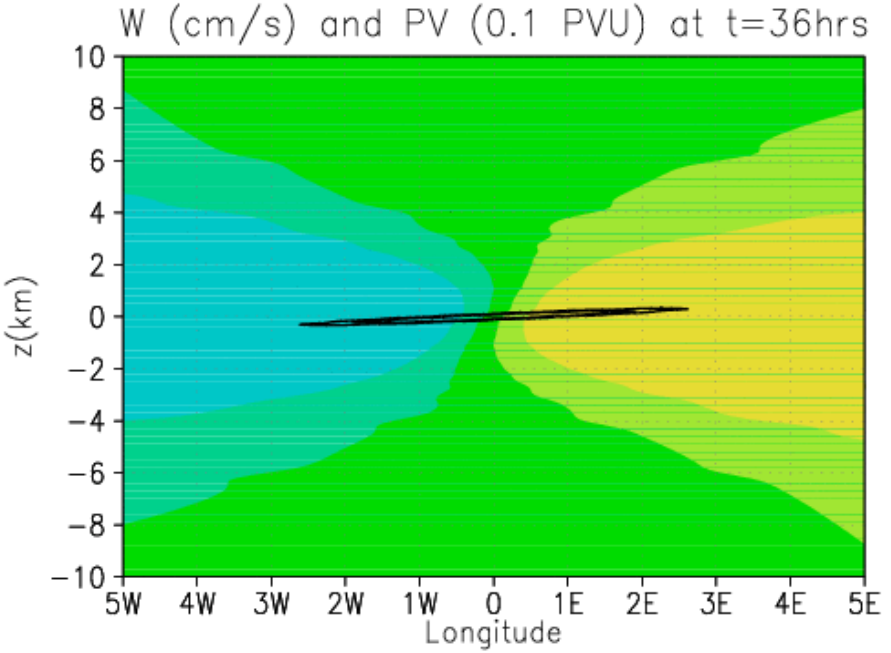

For the 2D results: *Lott, Plougonven and Vanneste, JAS 2010*.

Gravity waves from fronts and convection
4) GWs from front via a "smoking gun" approach

The complete solution can be reconstructed from a single monochromatic solution:

$$w'(x,y,z,t) = \hat{w}_0(k,l,\omega) W(\xi) e^{i(kx+ly-\omega t)}$$

$$\xi = \frac{k\Lambda}{f}(z-z') = \frac{k\overline{u}_0(z)-\omega}{f}$$

ξ=0 Ordinary critical level
(Intrinsic frequency=0)

ξ=-1,+1 Inertio critical levels
(Intrinsic frequency =$-f,+f$)

$(\partial_t + \overline{u}_0\partial_x)$
Advection

Its vertical structure satisfies the PV conservation Eq:

Disturbance PV

$$\xi\left(\left[-W_{\xi\xi}+\left(\frac{W_\xi}{\xi^2}\right)_\xi+\left(\frac{2i\nu W}{\xi^2}\right)_\xi-\frac{J(1+\nu^2)}{\xi^2}W\right]\right)=0$$

QG PV: $f\partial_z\theta' + \overline{\theta}_{0z}(\partial_x v' - \partial_y u')$

Richardson number $J=N^2/\Lambda^2$; Hor. Wavenumber ratio $\nu = l/k$

Gravity waves from fronts and convection
4) GWs from front via a "smoking gun" approach

The canonical solution $W(\xi)$ corresponds to a $\delta(\xi)$-PV distribution:

$$-W_{\xi\xi} + \left(\frac{W_\xi}{\xi^2}\right)_\xi + \left(\frac{2i\nu W}{\xi^2}\right)_\xi - \frac{J(1+\nu^2)}{\xi^2} W = \delta(\xi)$$

$\xi >> 1$: $E\,\xi^{1/2+i\mu}$ (upward GW)

$\xi > 1$: $E\,(1+\xi)^{-i\nu}\xi^{1/2+i\nu+i\mu} F(1-\xi^{-2})$

In $\xi=1$ the CL continuation links E with A and B

$0<\xi<1$: $(1+\xi)^{-i\nu}(A\,F'(\xi^2)+B\xi^3 F''(\xi^2))$

B and A such that $W_\xi/\xi^2(0^+) - W_\xi/\xi^2(0^-) = 1$

$-1<\xi<0$: $(1-\xi)^{+i\nu}(A^*\,F'^*(\xi^2)-B^*\xi^3 F''^*(\xi^2))$

$\xi << -1$: $E^*|\xi|^{1/2-i\mu}$ (downward GW)

F, F', and F'' Hypergeometric functions

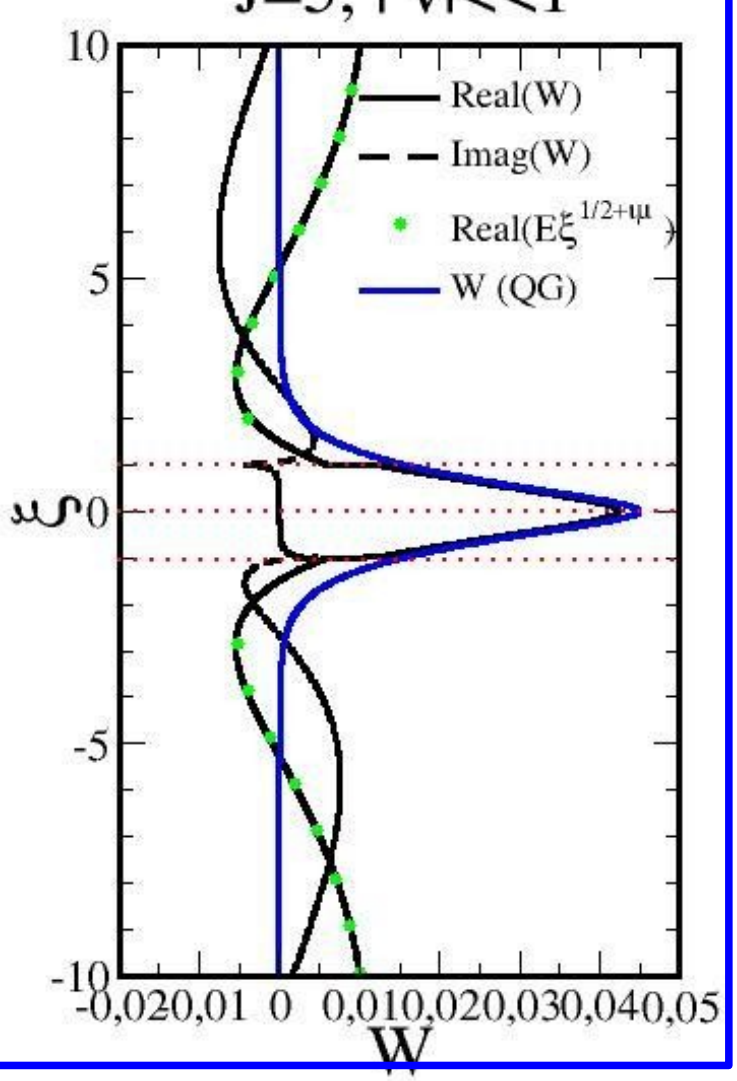

Gravity waves from fronts and convection
4) GWs from front via a "smoking gun" approach

$W(\xi)$ for various J, |ν|<<1, QG sols are in blue

$$\frac{1+\sqrt{J(1+\nu^2)}|\xi|}{2\left(J(1+\nu^2)\right)^{3/2}}e^{-\sqrt{J(1+\nu^2)}|\xi|}$$

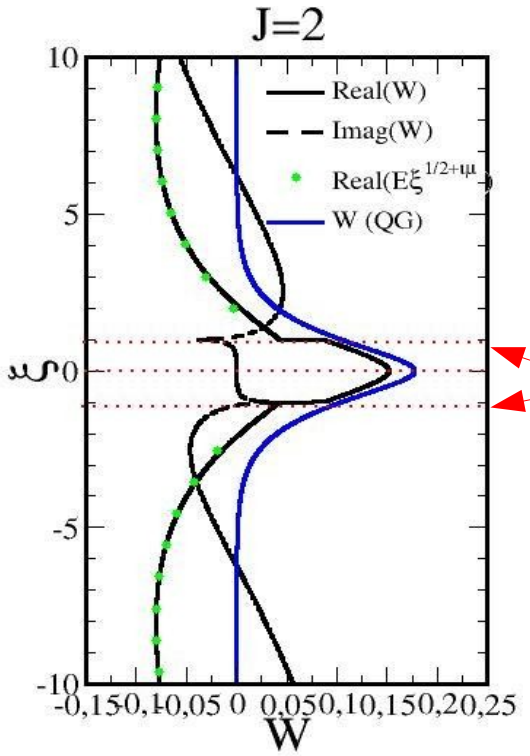

Inertial levels

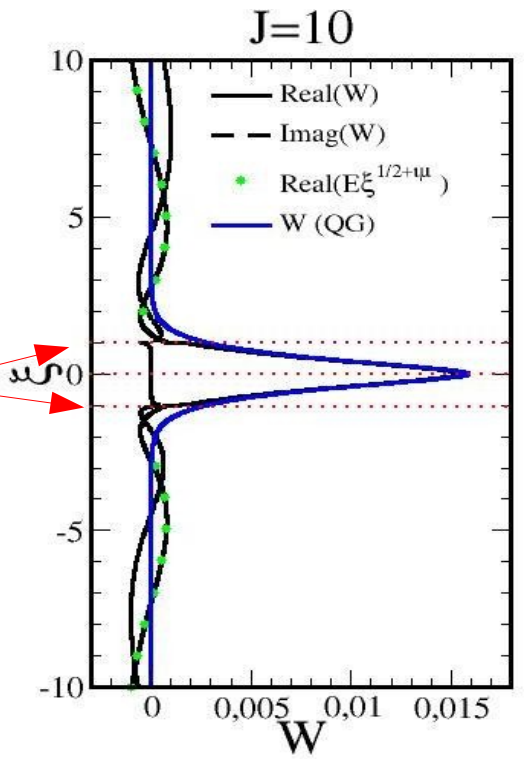

When -1<ξ<1 W is well predicted by the QG theory.

The QG value near the inertial levels (ξ=-1,+1) is

$$\frac{e^{-\sqrt{J(1+\nu^2)}}}{J(1+\nu^2)}$$

This could be the predictor of the GWs amplitude (If we assume that at the inertial level the signal becomes a GW and is not attenuated).

Gravity waves from fronts and convection
4) GWs from front via a “smoking gun” approach

The non dimensional Gravity Wave amplitude in the far field is <u>easy to predict:</u>

$$|E| \approx \frac{e^{-\pi/2\sqrt{J(1+\nu^2)}}}{2J(1+\nu^2)} \; e^{-\nu\pi/2}$$

~CL attenuation

~QG signal at the Inertio CL

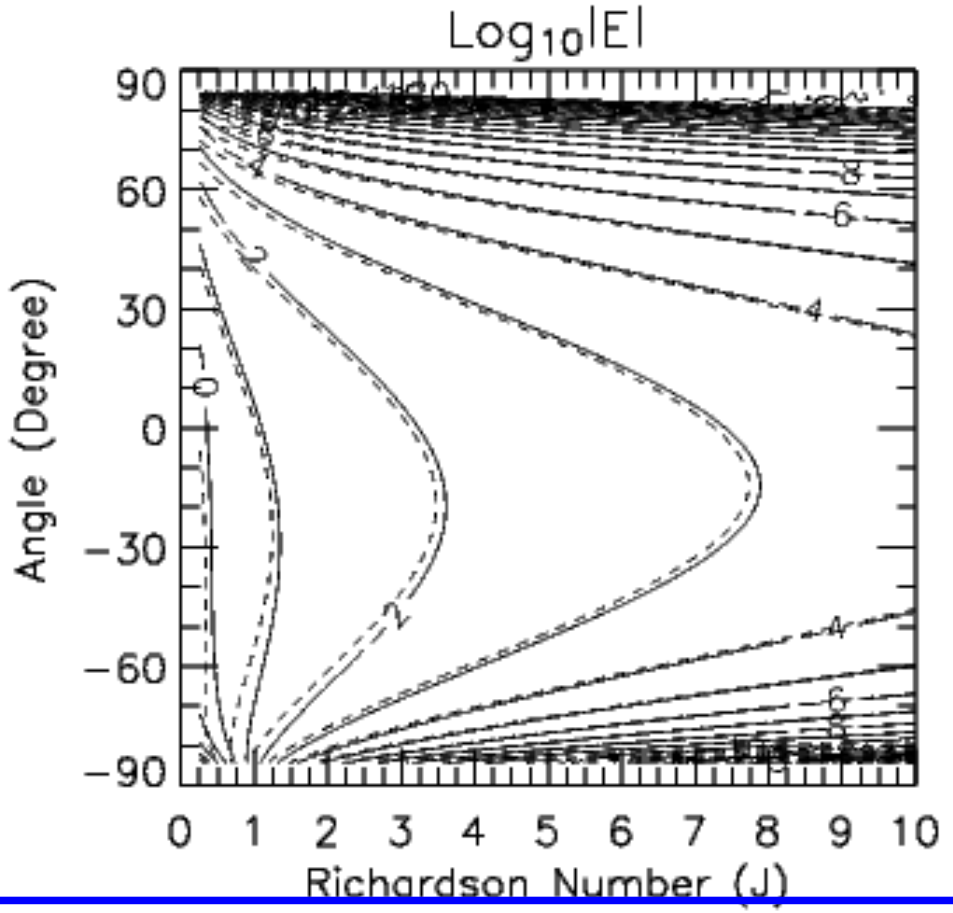

Exact values are solid

Approximation is dashed

Preferential emission at horizontal angles between -30° and -15°

when $1<J<10$

Gravity waves from fronts and convection
4) GWs from front via a “smoking gun” approach

General setup: A 3D (x,y,z) PV anomaly advected in a rotating (*f*=cte), stratified (BV freq *N*=cte) shear flow (vertical shear Λ=cte).

$wN^2 \sim f\Lambda v$

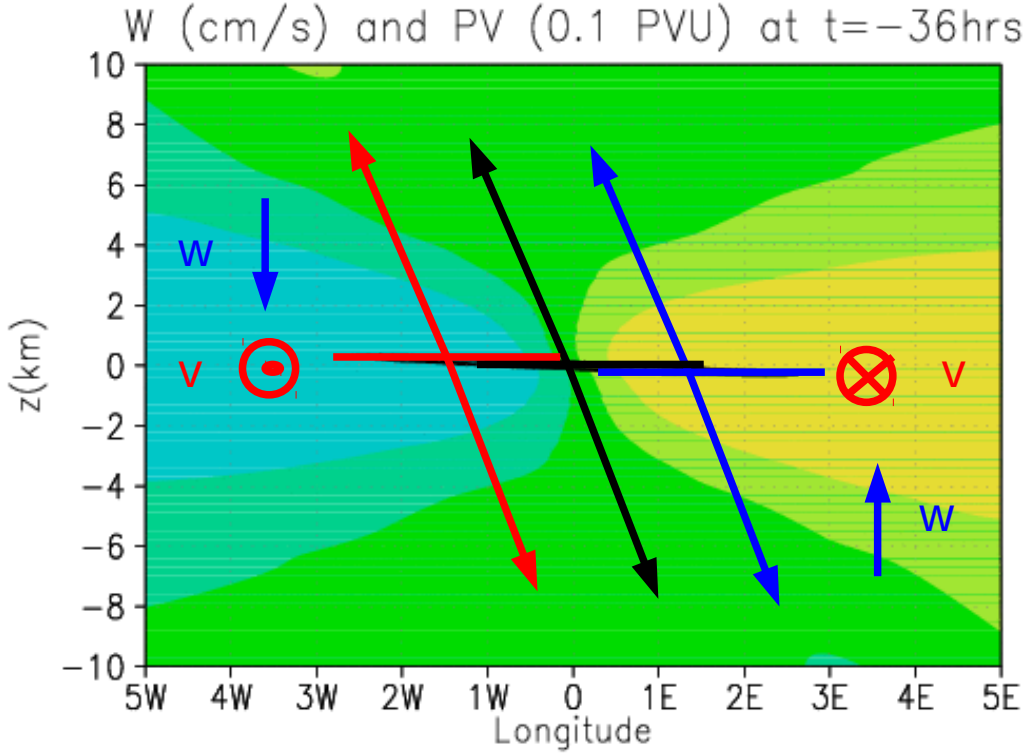

Gravity waves from fronts and convection
4) GWs from front via a “smoking gun” approach

General setup: A 3D (x,y,z) PV anomaly advected in a rotating (*f*=cte), stratified (BV freq *N*=cte) shear flow (vertical shear Λ=cte).

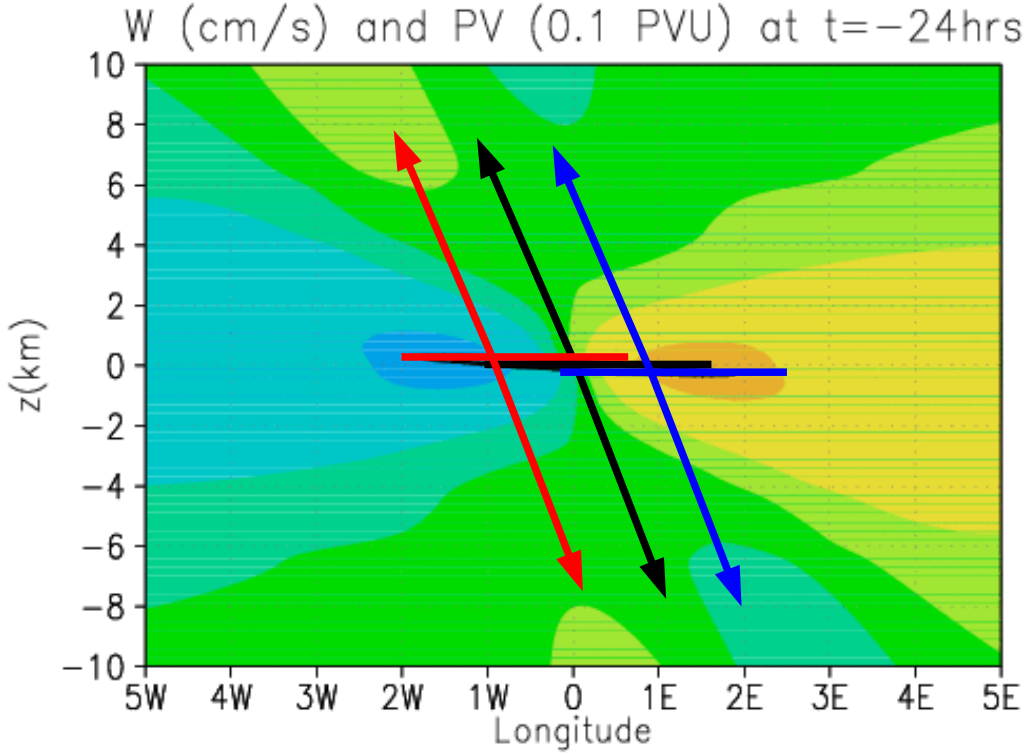

Gravity waves from fronts and convection
4) GWs from front via a “smoking gun” approach

General setup: A 3D (x,y,z) PV anomaly advected in a rotating (*f*=cte), stratified (BV freq *N*=cte) shear flow (vertical shear Λ=cte).

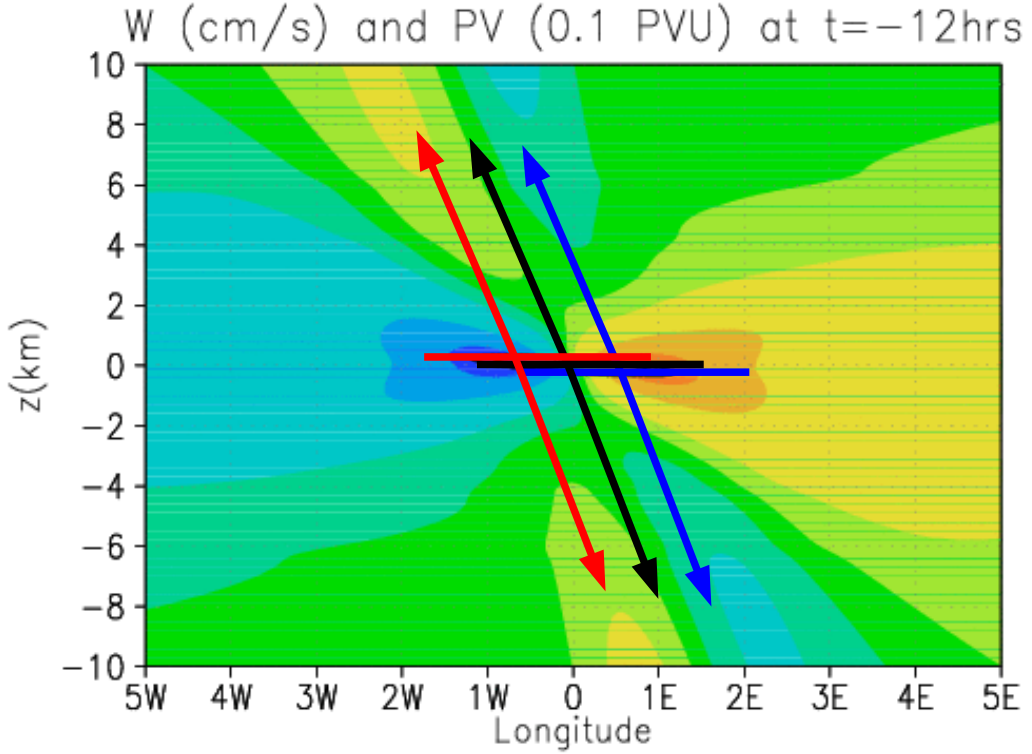

Gravity waves from fronts and convection
4) GWs from front via a “smoking gun” approach

General setup: A 3D (x,y,z) PV anomaly advected in a rotating (*f*=cte), stratified (BV freq *N*=cte) shear flow (vertical shear Λ=cte).

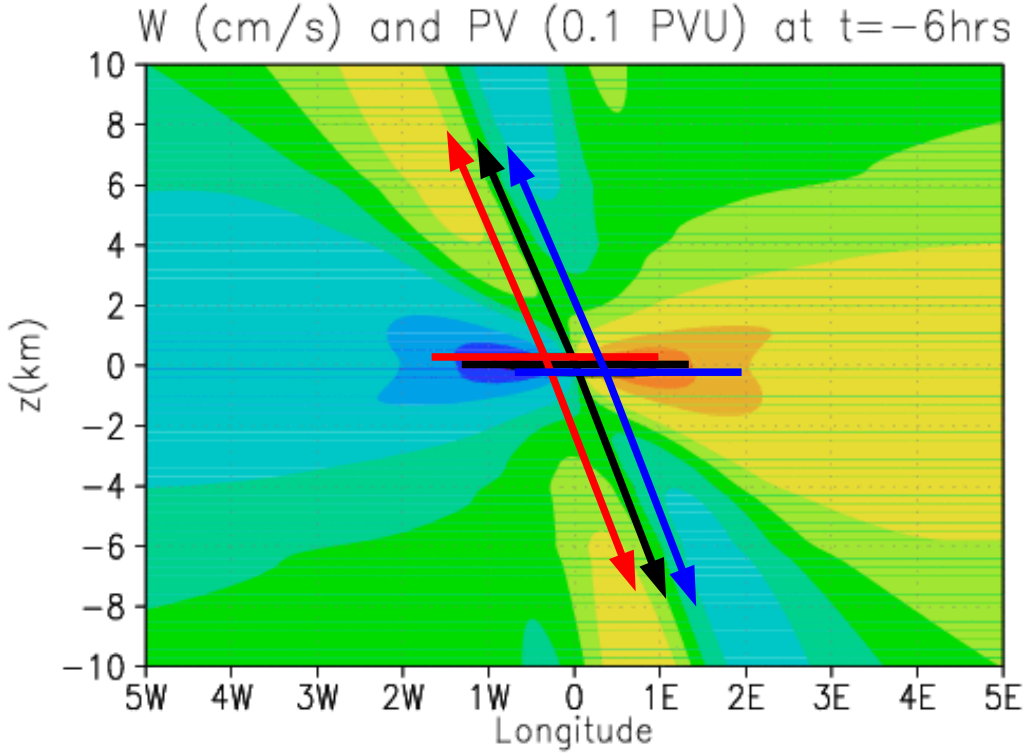

Gravity waves from fronts and convection
4) GWs from front via a “smoking gun” approach

General setup: A 3D (x,y,z) PV anomaly advected in a rotating (*f*=cte), stratified (BV freq *N*=cte) shear flow (vertical shear Λ=cte).

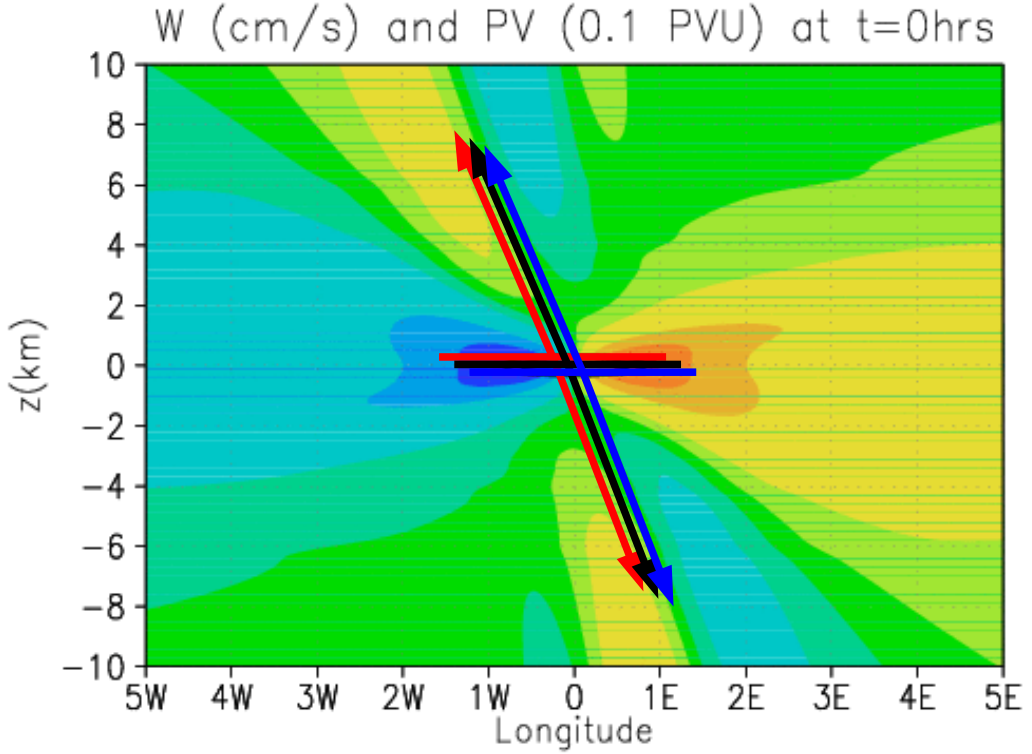

Gravity waves from fronts and convection
4) GWs from front via a “smoking gun” approach

General setup: A 3D (x,y,z) PV anomaly advected in a rotating (*f*=cte), stratified (BV freq *N*=cte) shear flow (vertical shear Λ=cte).

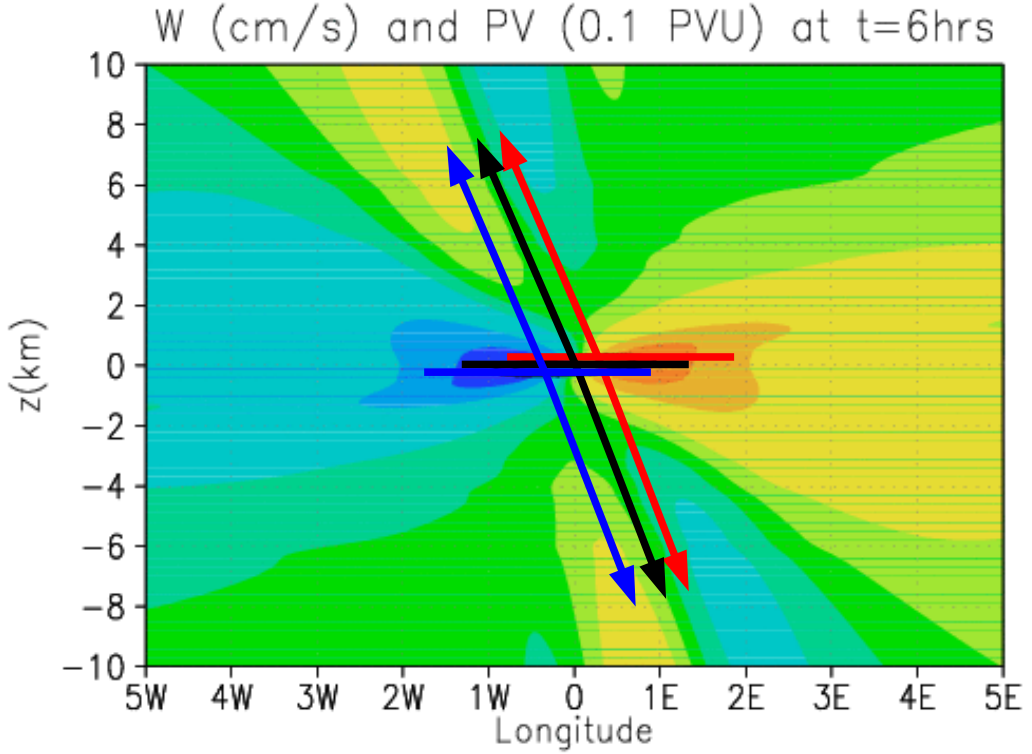

Gravity waves from fronts and convection
4) GWs from front via a “smoking gun” approach

General setup: A 3D (x,y,z) PV anomaly advected in a rotating (*f*=cte), stratified (BV freq *N*=cte) shear flow (vertical shear Λ=cte).

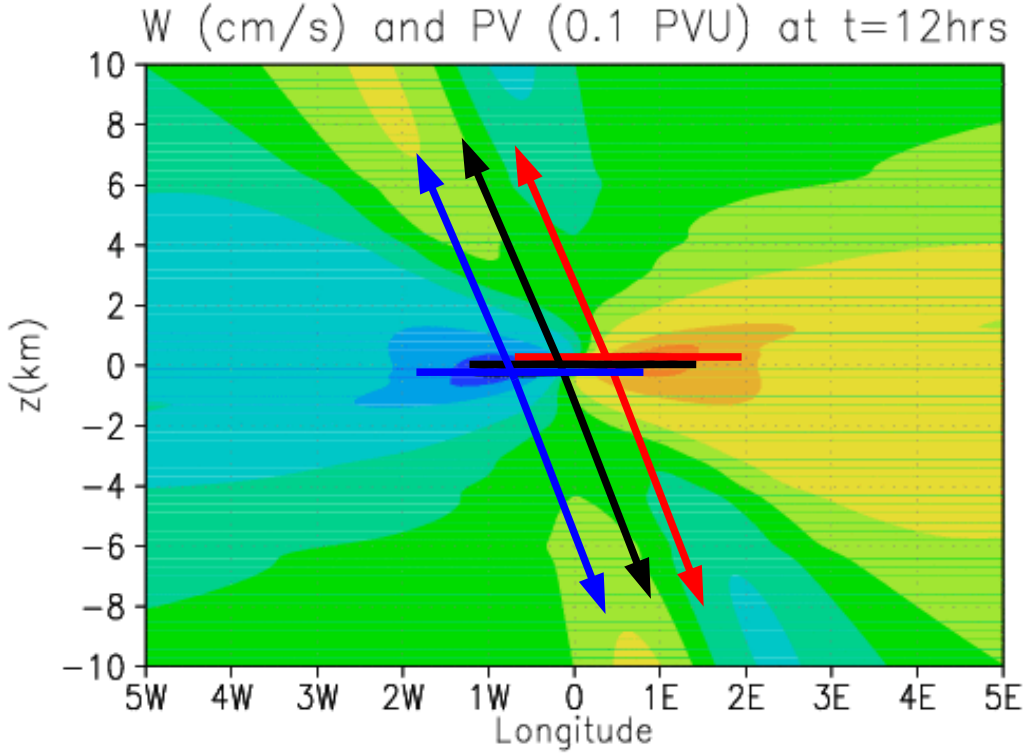

Gravity waves from fronts and convection
4) GWs from front via a “smoking gun” approach

General setup: A 3D (x,y,z) PV anomaly advected in a rotating (*f*=cte), stratified (BV freq *N*=cte) shear flow (vertical shear Λ=cte).

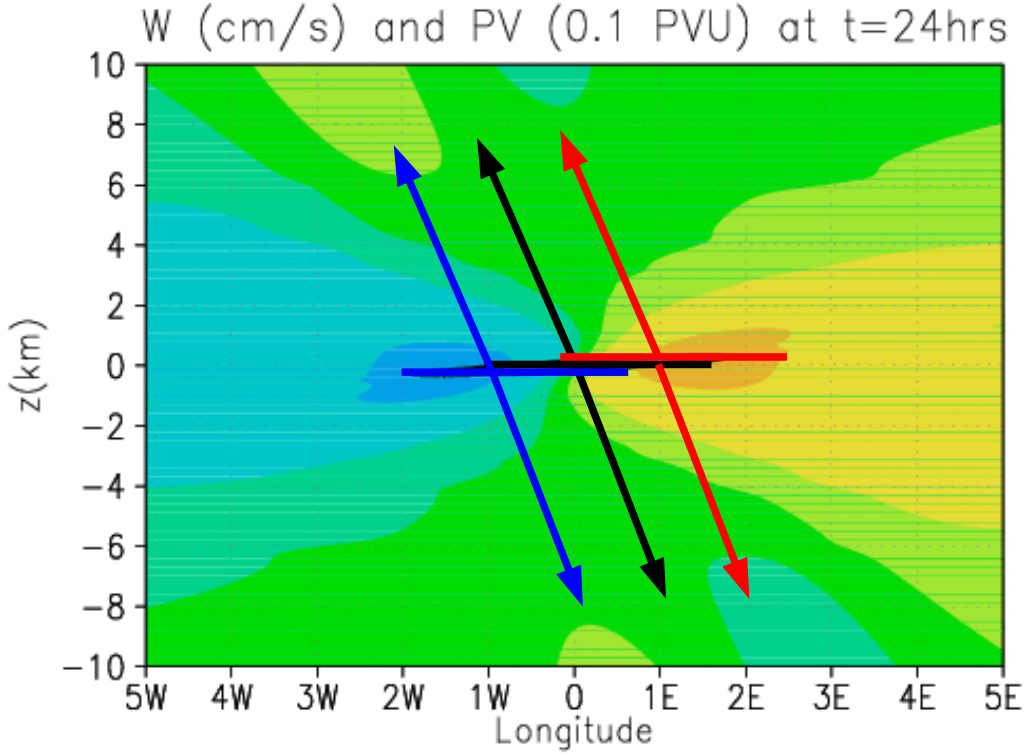

Gravity waves from fronts and convection
4) GWs from front via a “smoking gun” approach

General setup: A 3D (x,y,z) PV anomaly advected in a rotating (*f*=cte), stratified (BV freq *N*=ct e) shear flow (vertical shear Λ=cte).

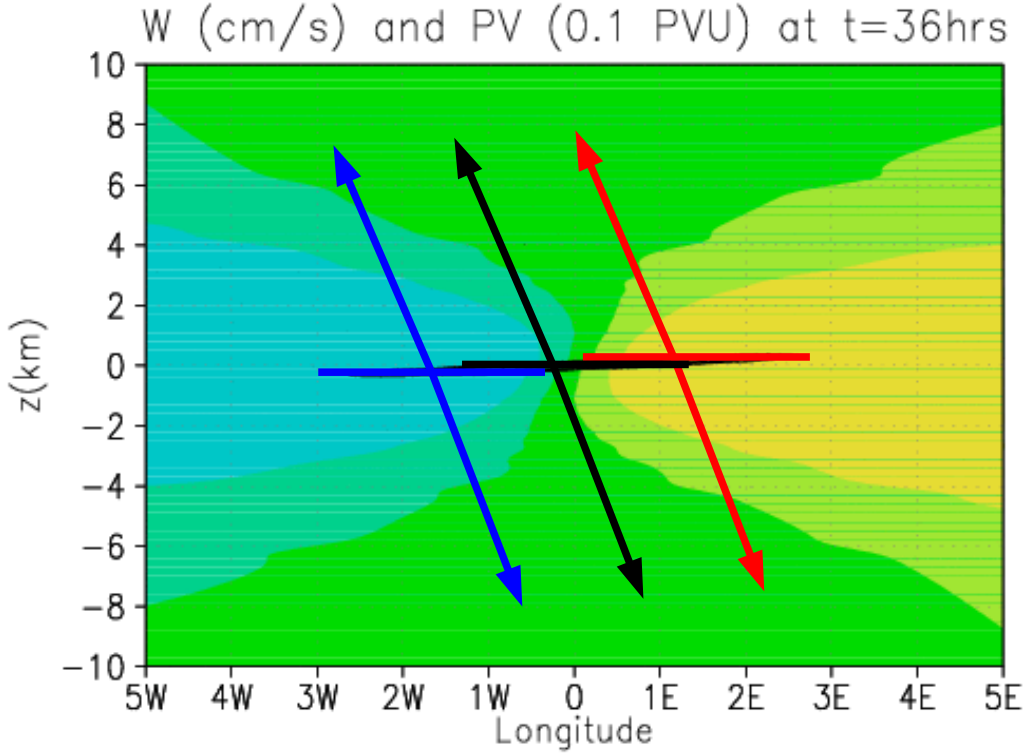

Gravity waves from fronts and convection
4) GWs from front via a “smoking gun” approach

The wave stress is predictable in closed analytical form:

$$F \approx \frac{\rho g^2}{f \theta^2 N^3} \left(\rho q_r \sigma_z\right)^2 \frac{e^{-\pi \frac{N}{\Lambda}}}{4}$$

PV anomaly

Characteristic depth of the PV anomaly

Valid for various PV distributions, and over long time scale (compared to the ½ hour interval at which subgrid-scale parameterisation routines are updated)

We next take for the PV q the GCM gridscale PV anomalies (as a measure of the subgrid scales one, again a “white” spectrum *hypothesis*)

For σ_z the GCM's layer depth.

Stochastic treatment of the k's, ω's, ect....

Gravity waves from fronts and convection
4) GWs from front via a “smoking gun” approach

The “smoking gun” theory predicts about the right amount of drag compared to a highly tuned globally spectral scheme (January, all in m/s/day)

Globally spectral scheme

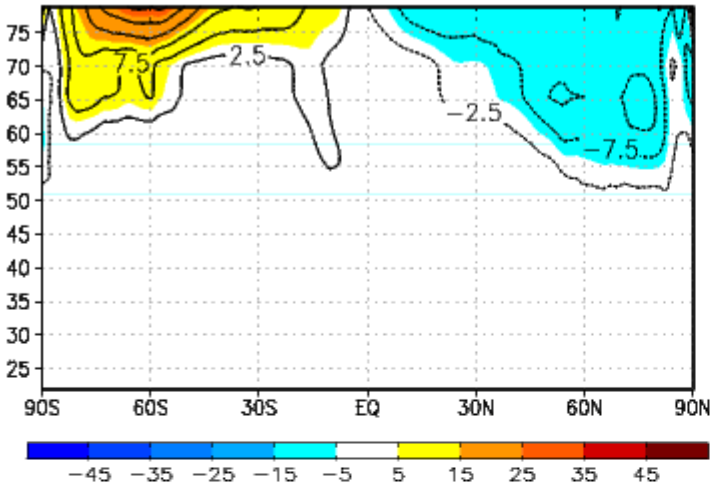

Smoking fronts

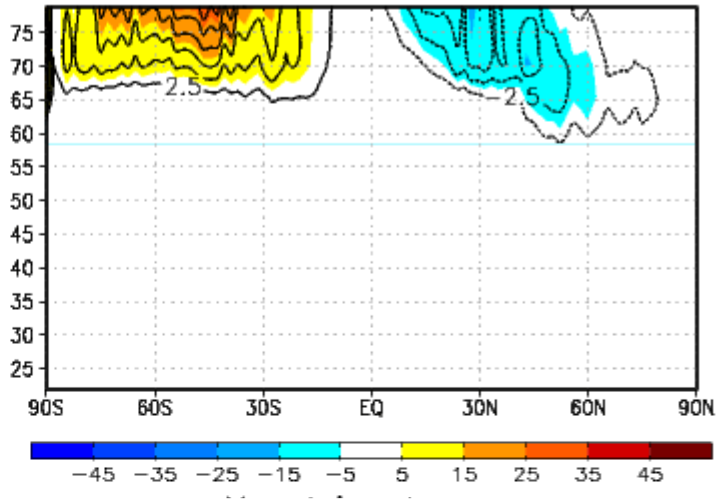

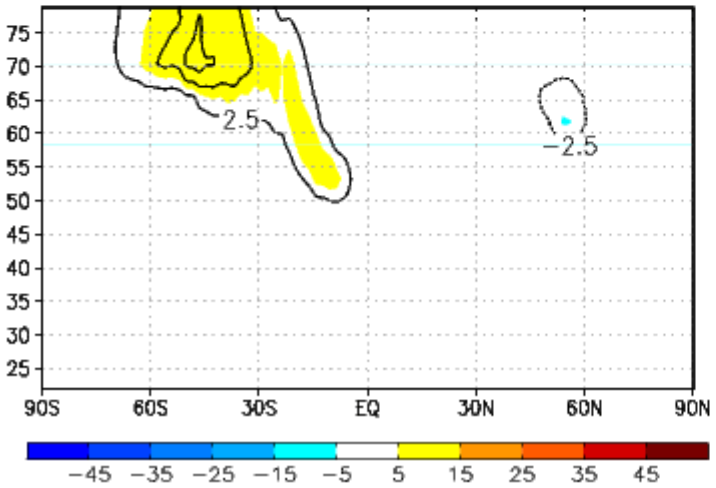

Convective GWs

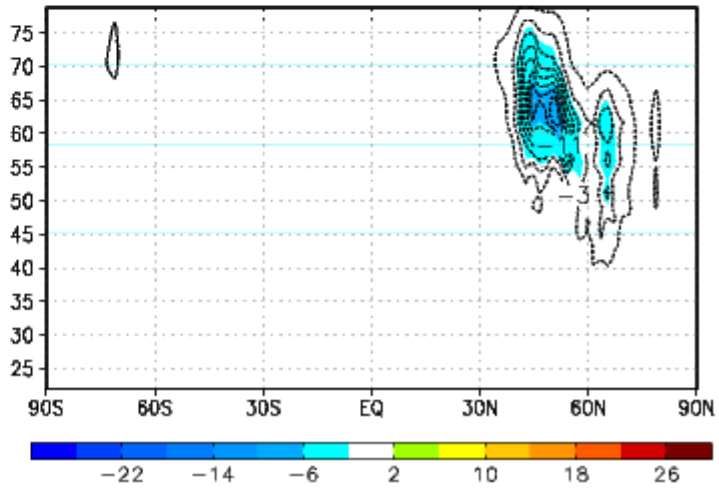

Mountains GWs

Gravity waves from fronts and convection
4) GWs from front via a “smoking gun” approach

Launched GWs stress amplitude, and $\|\vec{\nabla} T\|$ at 600hPa:

The waves predicted come from frontal zones

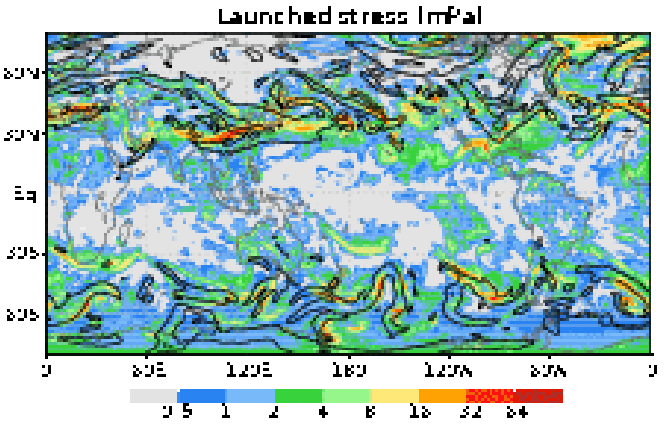

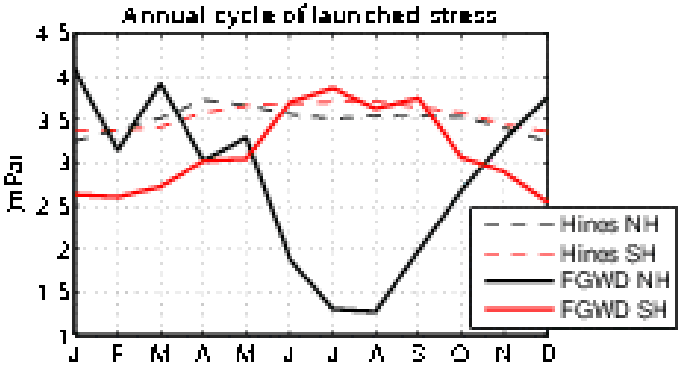

The wave stress now has an annual Cycle...

and realistic intemittency

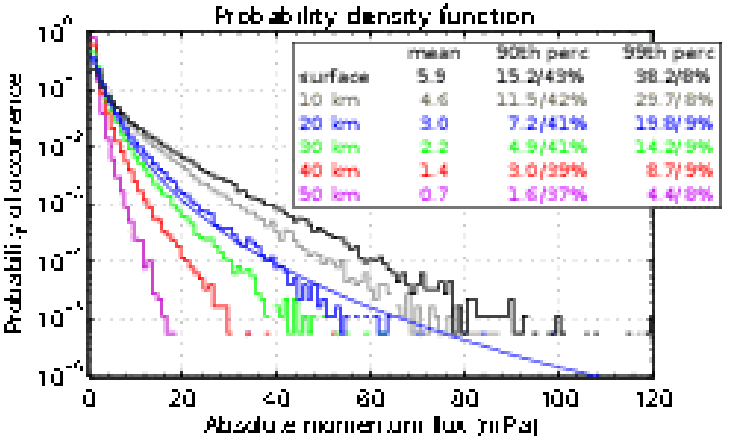

Gravity waves from fronts and convection
4) GWs from front via a “smoking gun” approach

Frontal GWs drag

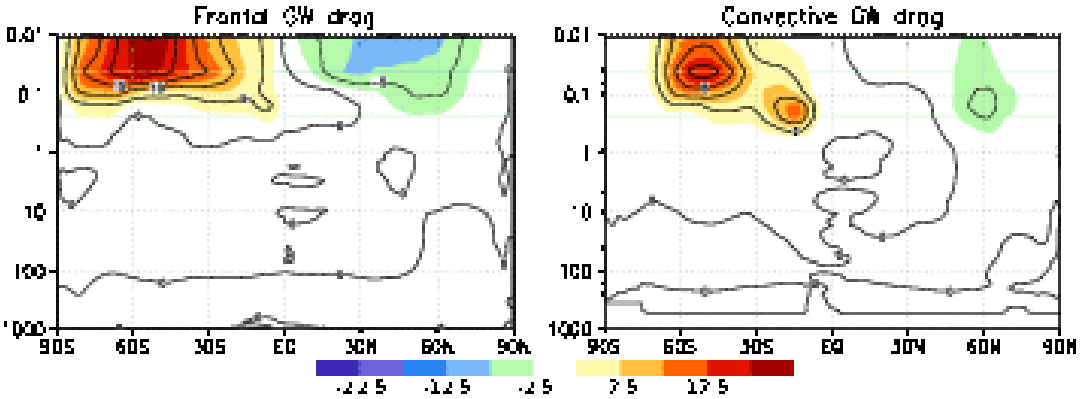

Convective GWs drag

Run with Hines
+
Convective waves

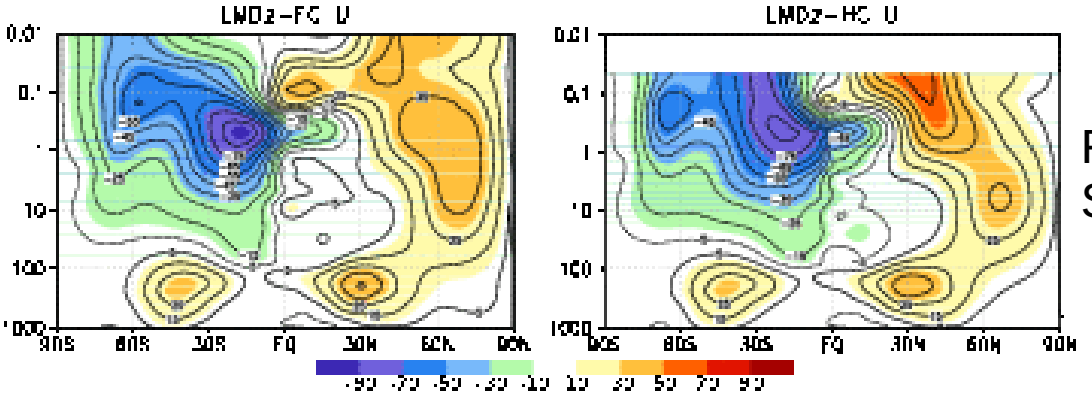

Frontal + Convective Stochastic GWs

ERA

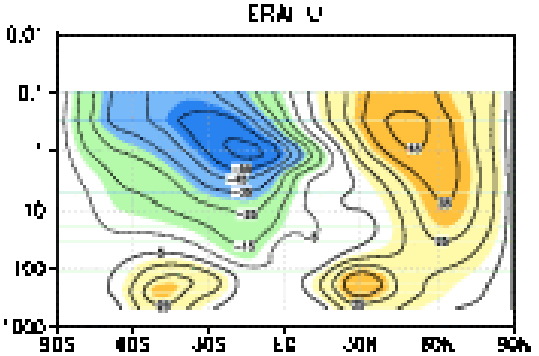

On line test with LMDz GCM
(de la Camara and Lott 2015)

Gravity waves from fronts and convection
4) GWs from front via a “smoking gun” approach

As we now have stronger annual cycles in the GWs launched fluxes, we need to look at element of the annual cycle in the stratospheric circulation that are still in error in present day GCMs.

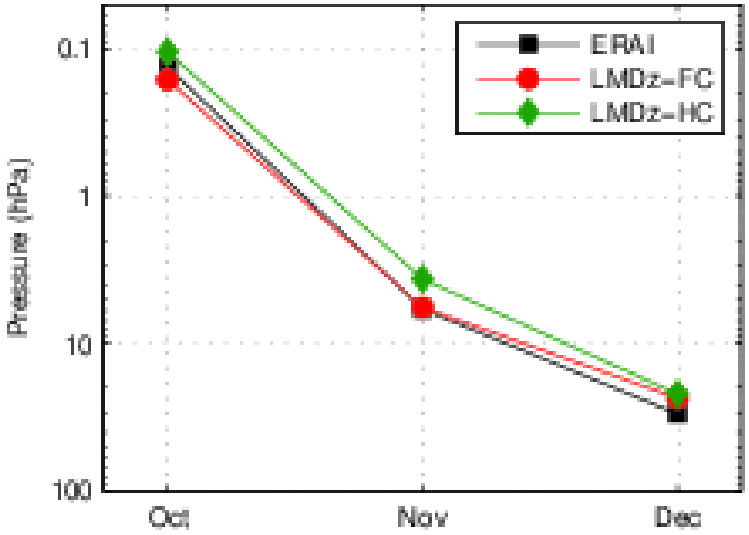

.

Descent of the zero zonal mean zonal wind lin at 60°S
(Timing of the SH vortex break-down)

On line test with LMDz GCM
(de la Camara and Lott 2015)

Gravity waves from fronts and convection
4) GWs from front via a “smoking gun” approach

4xCO2 +4K SST experiments, results for October
(month of the SH stratospheric vortex break-up)

Zonal mean zonal wind

Present Climate

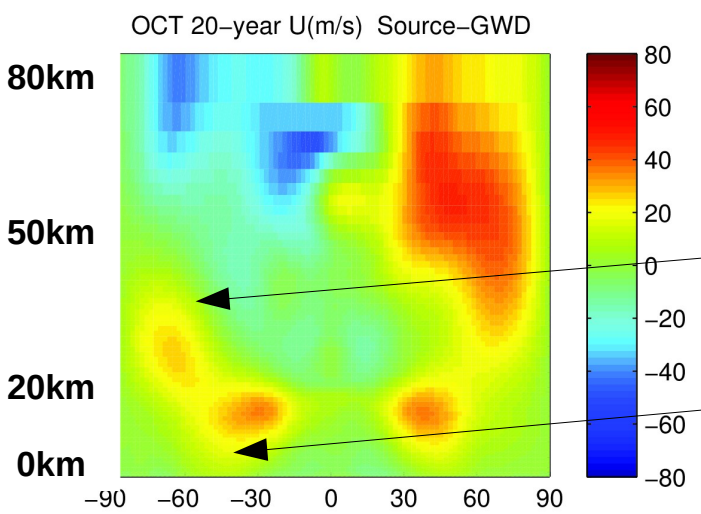

Future Climate

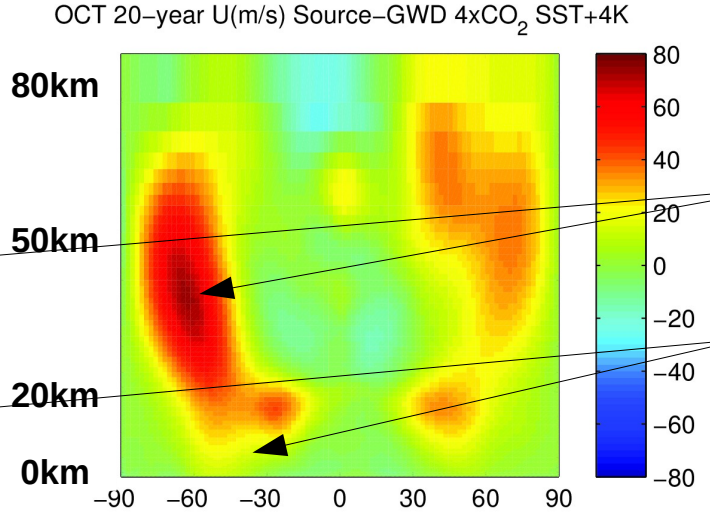

Break-up delayed

Surface Impact

Difference future-Present without GWs sources

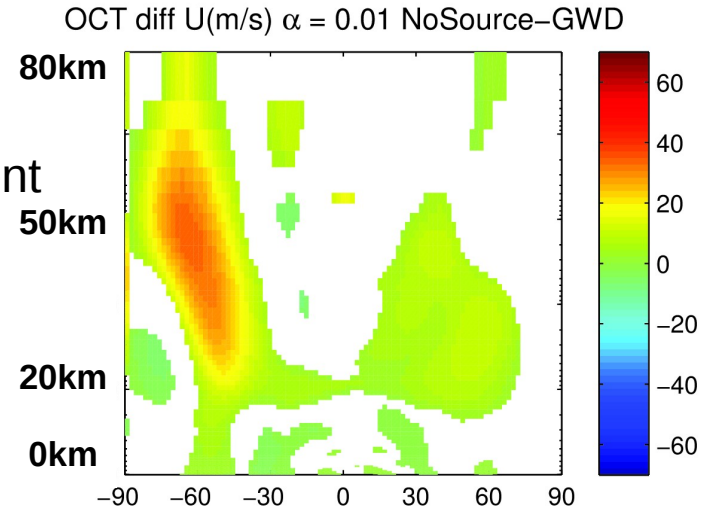

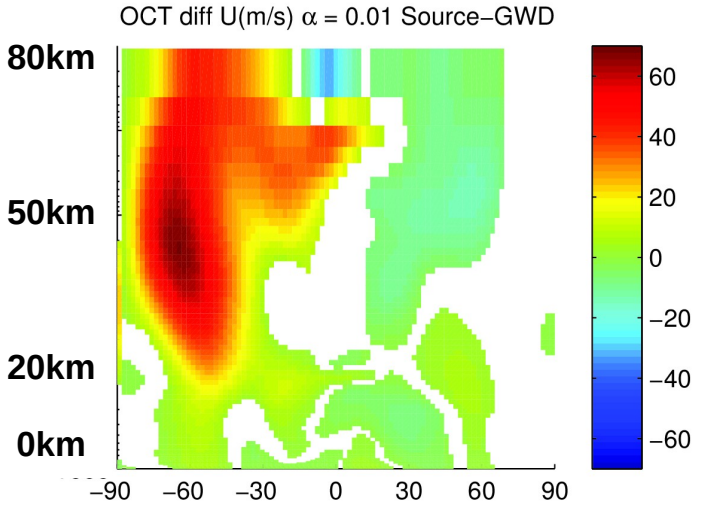

Difference future-present with GWs sources

Gravity waves from fronts and convection
5) Tests against observations

GWs from the scheme:

Offline runs using ERAI and GPCP data corresponding to the Concordiasi period.

Important: Satellite (partial) observations in the tropics support what is shown next.

www.lmd.polytechnique.fr/VORCORE/Djournal2/Journal.htm

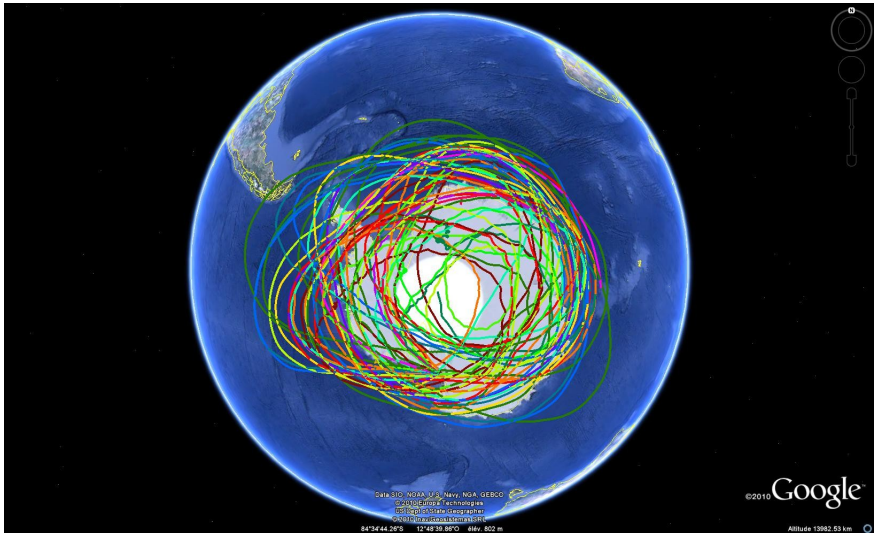

CONCORDIASI (2010)

Rabier et al. 2010 BAMS

19 super-pressure balloons launched from McMurdo, Antarctica, during Sep and Oct 2010.

The balloons were at ~ 20 km height.

Dataset of GW momentum fluxes *(as by Hertzog et al. 2008)*

www.lmd.polytechnique.fr/VORCORE/Djournal2/Journal.htm

Gravity waves from fronts and convection
5) Tests against observations

70's-90's observations (vertical soundings)

Long-term averages of vertical profiles show well-defined vertical wavenumber spectra

Van Zandt (1982), Fritts et al. (1988), Fritts&Lu (1993)

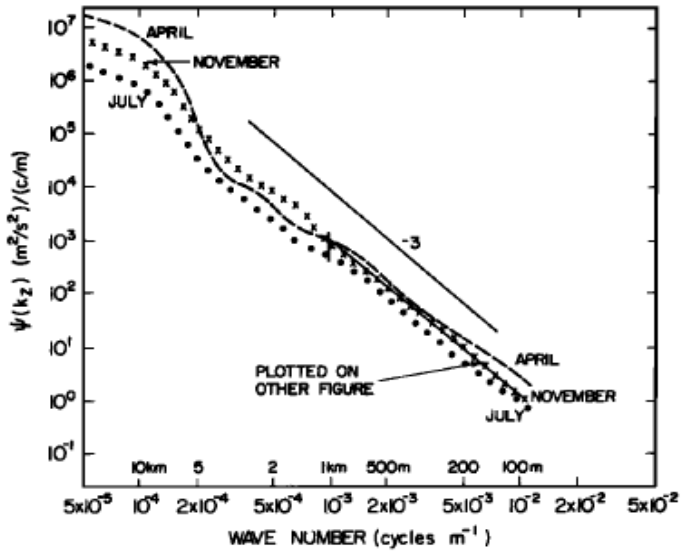

Dewan&Good 1986 JGR

Property used in global "spectral schemes"

Hines (1997), Warner&McIntyre (2001), Scinocca (2003)

Recent balloon and satellite obs.

Show intermittent GW fluxes

Hertzog et al. (2012).

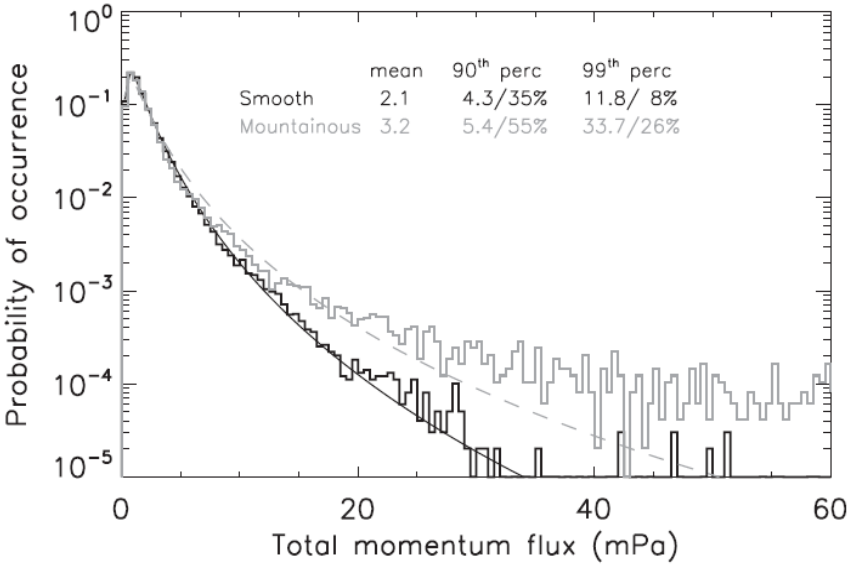

Hertzog et al. 2012 JAS

Property justifying stochastic schemes

Lott et al. (2012), Lott&Guez (2013)

Can these approach be reconciled?

Gravity waves from fronts and convection
5) Tests against observations

Intermittency of GW momentum flux

The stochastic scheme parameters can be tuned to produce fluxes as intermittent as in balloon observations.

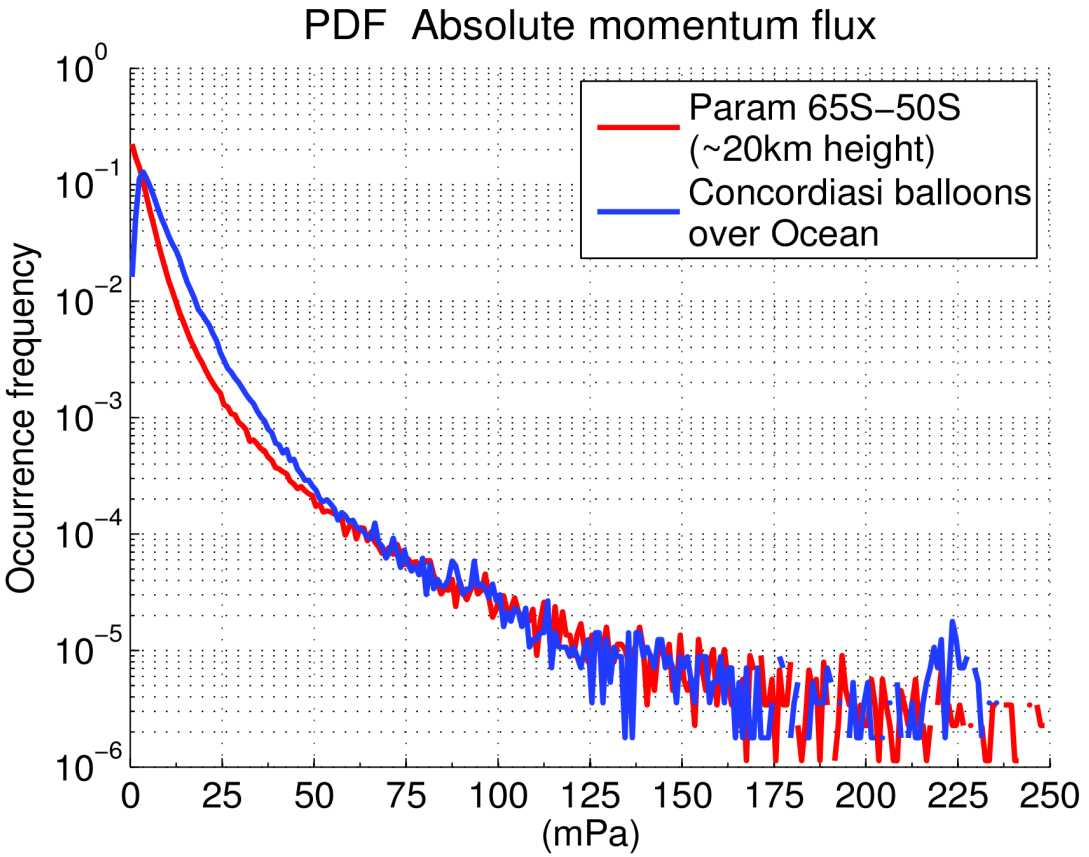

Remember that intermittency is important because it produces GW breaking at lower altitudes *(Lott&Guez 2013)*

de la Cámara et al. 2014, In press.

Gravity waves from fronts and convection
5) Tests against observations

Vertical spectra of GWs energy

The observed “universal spectra” can be obtained with a “multiwave scheme” as a superposition of individual periodograms of GW packets.

Average of periodograms

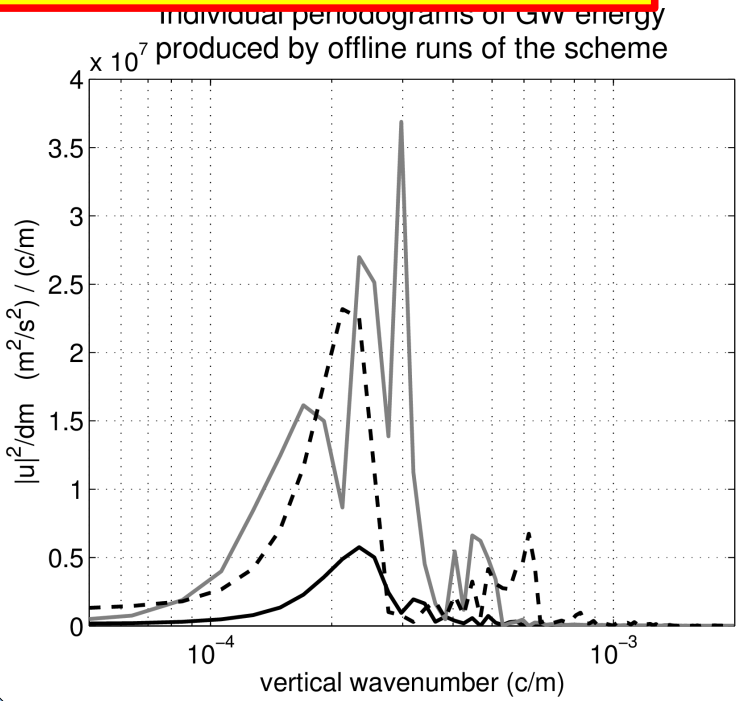

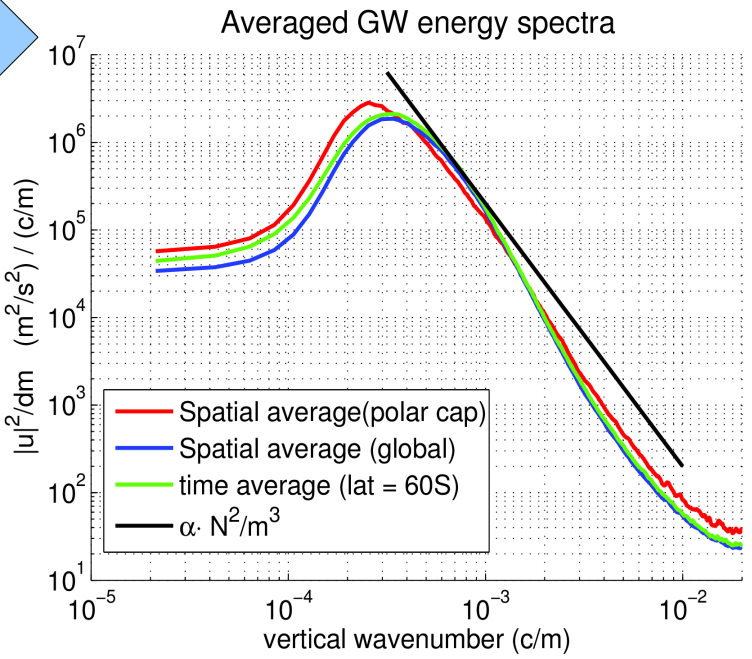

de la Cámara et al. 2014, In press

Gravity waves from fronts and convection
5) Tests against observations

What causes the intermittency?

Sources, like P^2 for convection or ξ^2 for fronts have lognormal distributions

(P precipitation, ξ relative vorticity)

For waves produced by PV see Lott et al.~(2012)

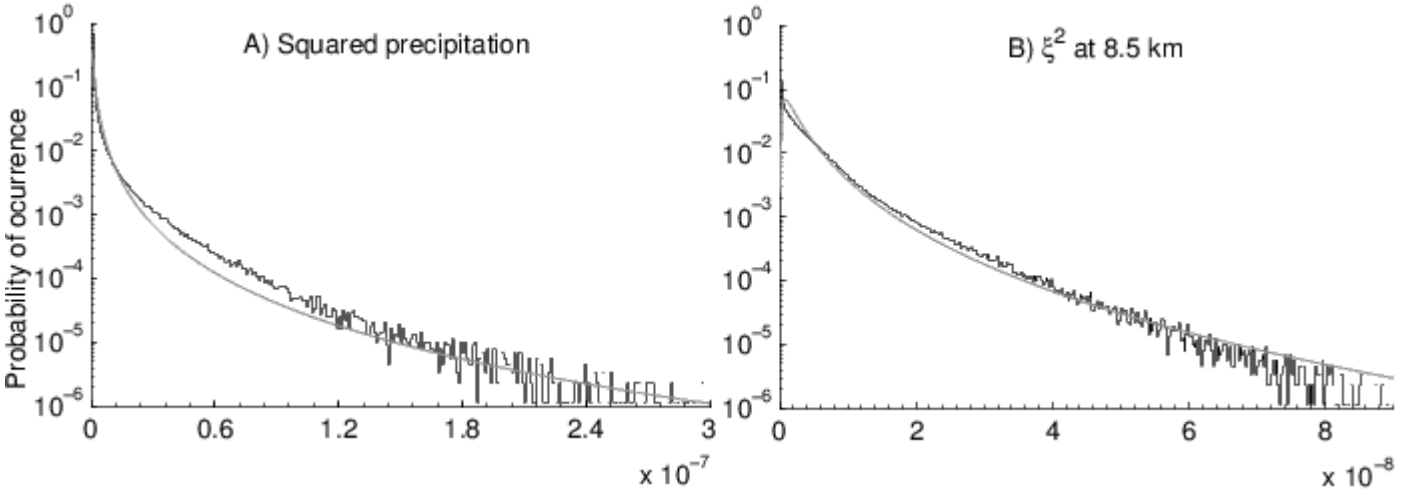

Results for intermittency suggest to relate the GWs to their sources

de la Cámara et al. 2014,Submitted

Gravity waves from fronts and convection
6) Perspectives

Will this physically based stochastic approaches increase the spread of climate Simulations?

For instance via an improvement of the year to year variability of the SH stratospheric winter vortex breakdown?

Now that the GWs are tied to the tropospheric weather, we can address their contribution to the climate change in the middle atmosphere

Does our unbalanced responses to upper-level PV anomalies modify the triggering of surface synoptic waves?

Extent stochastic methods to mountain waves?